Deposition of Centromeric Histone H3 Variant CENP-A/Cse4 into Chromatin Is Facilitated by Its C-Terminal Sumoylation

Kentaro Ohkuni,* Evelyn Suva,* Wei-Chun Au,* Robert L. Walker,* Reuben Levy-Myers,* Paul S. Meltzer,* Richard E. Baker,† and Munira A. Basrai*,1

*Genetics Branch, Center for Cancer Research, National Cancer Institute, National Institutes of Health, Bethesda, Maryland 20892, and †Department of Microbiology and Physiological Systems, University of Massachusetts Medical School, Worcester, Massachusetts 01655

ORCID ID: 0000-0001-9660-9299 (M.A.B.)

ABSTRACT Centromeric localization of CENP-A (Cse4 in *Saccharomyces cerevisiae*, CID in flies, CENP-A in humans) is essential for faithful chromosome segregation. Mislocalization of overexpressed CENP-A contributes to aneuploidy in yeast, flies, and humans, and is proposed to promote tumorigenesis in human cancers. Hence, defining molecular mechanisms that promote or prevent mislocalization of CENP-A is an area of active investigation. In budding yeast, evolutionarily conserved histone chaperones Scm3 and chromatin assembly factor-1 (CAF-1) promote localization of Cse4 to centromeric and noncentromeric regions, respectively. Ubiquitin ligases, such as Psh1 and Slx5, and histone chaperones (HIR complex) regulate proteolysis of overexpressed Cse4 and prevent its mislocalization to noncentromeric regions. In this study, we have identified sumoylation sites lysine (K) 215/216 in the C terminus of Cse4, and shown that sumoylation of Cse4 K215/216 facilitates its genome-wide deposition into chromatin when overexpressed. Our results showed reduced levels of sumoylation of mutant Cse4 K215/216R/A [K changed to arginine (R) or alanine (A)] and reduced interaction of mutant Cse4 K215/216R/A with Scm3 and CAF-1 when compared to wild-type Cse4. Consistent with these results, levels of Cse4 K215/216R/A in the chromatin fraction and localization to centromeric and noncentromeric regions were reduced. Furthermore, in contrast to *GAL-CSE4*, which exhibits Synthetic Dosage Lethality (SDL) in *psh1*Δ, *slx5*Δ, and *hir2*Δ strains, *GAL-cse4 K215/216R* does not exhibit SDL in these strains. Taken together, our results show that deposition of Cse4 into chromatin is facilitated by its C-terminal sumoylation.

KEYWORDS Sumoylation; Cse4; Chromatin assembly factor-1; Scm3; *Saccharomyces cerevisiae*; Centromere; CENP-A; Kinetochore; Budding yeast; Psh1

ANEUPLOIDY is a hallmark of many cancers and a significant driver of tumorigenesis. Aneuploidy, observed in 90% of solid tumors, is caused by chromosomal instability (CIN), characterized by the unequal distribution of chromosomes into two daughter cells and/or structural rearrangements of the genome. One of the key determinants for chromosomal stability is the centromere, which serves as a site for kinetochore assembly and mediates kinetochore-microtubule attachment and spindle assembly checkpoint function. The incorporation of the evolutionarily conserved centromeric histone H3 variant Cse4 (Cnp1 in *Schizosaccharomyces pombe*, CID in *Drosophila melanogaster*, and CENP-A in humans) into centromeric chromatin is essential for kinetochore assembly and chromosomal stability (Kitagawa and Hieter 2001; Biggins 2013; McKinley and Cheeseman 2016).

The evolutionarily conserved CENP-A specific histone chaperone Scm3 in *Saccharomyces cerevisiae* and *S. pombe* [CAL1 in *D. melanogaster*, Holliday Junction Recognition Protein (HJURP) in humans] promotes the centromeric localization of Cse4 and Cnp1, respectively (Camahort *et al.* 2007; Mizuguchi *et al.* 2007; Stoler *et al.* 2007; Pidoux *et al.* 2009; Williams *et al.* 2009). Other chaperones besides Scm3

doi: https://doi.org/10.1534/genetics.120.303090
Manuscript received August 21, 2019; accepted for publication February 26, 2020; published Early Online February 28, 2020.
Supplemental material available at figshare: https://doi.org/10.25386/genetics.11899908.
[1]Corresponding author: Genetics Branch, Center for Cancer Research, National Cancer Institute, National Institutes of Health, 41 Medlars Dr., Room B624, Bethesda, MD 20892. E-mail: basraim@nih.gov

facilitate the deposition of overexpressed Cse4 when the balance of H3 and Cse4 is altered. For example, the evolutionarily conserved replication dependent Chromatin Assembly Factor 1 (CAF-1) in *S. cerevisiae* promotes localization of overexpressed Cse4 to centromeres (Hewawasam *et al.* 2018). The CAF-1 ortholog Mis16 in *S. pombe* and RbAp46/48 in humans and *D. melanogaster* contribute to efficient CENP-A loading to centromeres (Fujita *et al.* 2007; Pidoux *et al.* 2009; Williams *et al.* 2009; Boltengagen *et al.* 2016). In *S. cerevisiae*, CAF-1 complex not only promotes localization of overexpressed Cse4 to centromeres, but also contributes to the mislocalization of Cse4 to noncentromeric regions (Hewawasam *et al.* 2018). In humans, the transcription-coupled histone H3/H4 chaperone DAXX/ATRX promotes mislocalization of CENP-A to ectopic regions (Lacoste *et al.* 2014; Athwal *et al.* 2015; Shrestha *et al.* 2017).

Previous studies have shown that mislocalization of overexpressed CENP-A contributes to aneuploidy in yeast, flies, and human cells (Collins *et al.* 2004; Heun *et al.* 2006; Moreno-Moreno *et al.* 2006; Au *et al.* 2008; Shrestha *et al.* 2017). Furthermore, many cancers exhibit elevated CENP-A messenger RNA levels, and this correlates with poor patient survival and increased risk of disease progression (Tomonaga *et al.* 2003; Amato *et al.* 2009; Hu *et al.* 2010; Li *et al.* 2011; Wu *et al.* 2012; Lacoste *et al.* 2014; Athwal *et al.* 2015; Sun *et al.* 2016). Hence, understanding pathways that promote and prevent mislocalization of CENP-A is an area of active research.

In *S. cerevisiae*, post-translational modifications such as ubiquitination and sumoylation of Cse4, and histone chaperones such as the HIR complex, regulate proteolysis and cellular levels of Cse4, preventing its mislocalization to noncentromeric regions, and thereby maintaining chromosomal stability (Collins *et al.* 2004; Hewawasam *et al.* 2010; Ranjitkar *et al.* 2010; Lopes da Rosa *et al.* 2011; Ohkuni *et al.* 2016; Cheng *et al.* 2017; Ciftci-Yilmaz *et al.* 2018). Our recent study with a genome-wide screen using synthetic genetic array with conditional mutant alleles of essential genes identified a role of F-box proteins Met30 and Cdc4 of the Skp1, Cullin, F-box (SCF) complex in the proteolysis of endogenous Cse4 to prevent its mislocalization and promote chromosome stability (Au *et al.* 2020). We have previously shown that Cse4 is a substrate for sumoylation as well as ubiquitination (Ohkuni *et al.* 2016). We determined that the small ubiquitin-like modifier (SUMO)-targeted ubiquitin ligase Slx5 regulates proteolysis of Cse4 and prevents its mislocalization to noncentromeric regions (Ohkuni *et al.* 2016). Most SUMO substrates are modified at lysine residues found in the consensus motif Ψ-K-x-D/E (Ψ is a hydrophobic residue, K is the lysine to conjugated to SUMO, x is any amino acid, D or E is an acidic residue) (Rodriguez *et al.* 2001; Sampson *et al.* 2001; Bernier-Villamor *et al.* 2002). We recently reported that sumoylation of K65 (64-S**K**SD-67) in the N terminus of Cse4 promotes its interaction with Slx5 and regulates proteolysis of Cse4 to prevent its mislocalization for faithful chromosome segregation (Ohkuni *et al.* 2018).

In this study, we have identified and defined a role for sumoylation of Cse4 K215/K216 (214-M**KK**D-217) in the C terminus that is functionally distinct from the N-terminal sumoylation of Cse4 K65. We report that, unlike Cse4 K65R, defects in proteolysis are not observed for Cse4 K215/216R/A and Cse4 K215/216R/A is not mislocalized to noncentromeric regions. Our results show defects in the interaction of Cse4 K215/216R/A with Scm3 and CAF-1 and reduced levels of Cse4 K215/216R/A at centromeric and noncentromeric regions, compared to wild-type Cse4. Furthermore, in contrast to *GAL-CSE4*, which exhibits Synthetic Dosage Lethality (SDL) in *psh1*Δ, *slx5*Δ, and *hir2*Δ strains, *GAL-cse4 K215/216R* does not exhibit SDL in these strains. We conclude that Cse4 K215/K216 sumoylation promotes its interaction with CAF-1 and Scm3, and this facilitates the deposition of Cse4 into chromatin. Our studies with the triple mutant *cse4 K65/215/216R* show that the biological role of Cse4 K215/216 sumoylation is independent of the role of Cse4 K65 sumoylation.

Materials and Methods

Yeast strains and plasmids

Supplemental Material, Tables S1 and S2 describe the genotypes of yeast strains and plasmids used for this study, respectively.

Sumoylation assay and co-immunoprecipitation

Cell lysates were prepared from 50 ml culture of strains grown to exponential phase in raffinose/galactose (2%) medium for 2–4 hr to induce expression of Cse4 from the *GAL* promoter. Cells were pelleted, rinsed with sterile water, and suspended in 0.5 ml of guanidine buffer (0.1 M Tris-HCl at pH 8.0, 6.0 M guanidine chloride, 0.5 M NaCl) for sumoylation assay, or 0.5 ml of IP lysis buffer (50 mM Tris-HCl at pH 8.0, 5 mM EDTA, 1% Triton X-100, 150 mM NaCl, 50 mM NaF, 10 mM β-glycerophosphate, 1 mM PMSF, 1x protease inhibitor cocktail) for co-immunoprecipitation (Co-IP). Cells were homogenized with Matrix C (MP Biomedicals) using a bead beater (FastPrep-24 5G; MP Biomedicals). Cell lysates were clarified by centrifugation at 6000 rpm for 5 min and protein concentration was determined using a DC protein assay kit (Bio-Rad, Hercules, CA). Samples containing equal amounts of protein were brought to a total volume of 1 ml with appropriate buffer.

In vivo sumoylation was assayed in crude yeast extracts using nickel-nitrilotriacetic acid (Ni-NTA) agarose beads to pull down His-HA-tagged Cse4 as described previously (Ohkuni *et al.* 2015), with modifications. Cell lysates were incubated with 100 μl of Ni-NTA superflow beads (30430; Qiagen, Valencia, CA) overnight at 4°. After being washed with guanidine buffer one time and with breaking buffer (0.1 M Tris-HCl at pH 8.0, 20% glycerol, 1 mM PMSF) five times, beads were incubated with 2 × Laemmli buffer including imidazole at 100° for 10 min. The protein samples were analyzed by SDS-PAGE and Western blotting. Co-IPs were performed as described previously (Ohkuni *et al.* 2018), with

modifications. Cell lysates were incubated with 20 μl of Anti-FLAG M2 Affinity Gel (A2220; Sigma, St. Louis, MO) for 2 hr at 4°. After being washed with IP lysis buffer three times, beads were incubated with 2 × Laemmli buffer at 100° for 5 min. The protein samples were analyzed by SDS-PAGE and Western blotting.

Protein stability assay

Protein stability assays were performed as described previously (Ohkuni *et al.* 2016). Cells were grown to logarithmic phase of growth in a 2% raffinose synthetic complete medium. Galactose was added to the media to a final concentration of 2% to induce Cse4 expression from the *GAL* promoter for 2 hr. Cycloheximide (CHX) and glucose were then added to final concentrations of 10 μg/ml and 2%, respectively. Samples were taken at the indicated time points and levels of Cse4 were quantified by Western blot analysis. Multiple independent measurements were made, and means±SDs are given on the applicable figures, with the number of replicates given in parentheses.

Subcellular fractionation assay

Cells were grown to logarithmic phase of growth in a 2% raffinose synthetic complete medium at 30°. Galactose was added to the media to a final concentration of 2% to induce Cse4 expression from the *GAL* promoter for 4 hr. Subcellular fractionation was performed as described previously (Au *et al.* 2008) with minor modifications. Whole cell extracts (WCEs) were prepared from lysates before the sucrose gradient centrifugation.

SDS-PAGE, Western blotting, antibodies, and quantification

SDS-PAGE and Western blotting were performed as described previously (Ohkuni *et al.* 2018). Primary antibodies were as follows: anti-HA (12CA5) mouse (11583816001; Roche), anti-HA rabbit (H6908; Sigma), anti-Smt3 rabbit (y-84) (sc-28649; Santa Cruz Biotechnology), anti-Tub2 rabbit (Basrai laboratory), anti-Pgk1 mouse (459250; Invitrogen, Carlsbad, CA), anti-H3 rabbit (ab1791; Abcam), anti-FLAG mouse (F3165; Sigma), anti-FLAG rabbit (F7425; Sigma), and anti-Cse4 rabbit (Strahl laboratory). Secondary antibodies were ECL mouse IgG, HRP-linked whole Ab (NA931V; GE Healthcare Life Sciences) or ECL rabbit IgG, HRP-linked whole Ab (NA934V; GE Healthcare Life Sciences). Protein levels were quantified using Gene Tools software (version 3.8.8.0) from SynGene (Frederick, MD), or Image Lab software (version 6.0.0) from Bio-Rad.

Chromosome loss assay

Chromosome loss assays were performed as described previously (Spencer *et al.* 1990; Au *et al.* 2008). Briefly, strains containing a nonessential reporter chromosome (RC) were plated on synthetic defined medium with limiting adenine to allow loss of the nonessential RC and incubated at 30° for 5 days. Loss of the RC results in red sectors in an otherwise white colony. At least 4000 colonies were assayed for each strain.

Chromatin immunoprecipitation quantitative PCR and chromatin immunoprecipitation sequencing experiments

Cells were grown to logarithmic phase of growth in a 2% raffinose synthetic complete medium at 30°. Galactose was added to the media to a final concentration of 2% to induce Cse4 expression from the *GAL* promoter for 2 hr at 30°. Then, 220 OD_{600} of cells were fixed in 1% formaldehyde for 20 min at 30°, quenched with glycine (final concentration 0.4 M) for 5 min, and washed three times with cold TBS (20 mM Tris-HCl at pH 7.5, 150 mM NaCl). Cells were then suspended in FA buffer (50 mM HEPES at pH 7.5, 150 mM NaCl, 1 mM EDTA, 1% Triton X-100, 0.1% Na-deoxycholate, 1 mM PMSF, 1 × protease inhibitor cocktail), homogenized 2 times for 40 sec with Matrix C (MP Biomedicals) using a bead beater (FastPrep-24 5G; MP Biomedicals), and centrifuged to discard the supernatant. The pellets were resuspended in FA buffer, vortexed, and centrifuged to collect the crude chromatin. The pellets were resuspended in FA buffer again and the lysates were sonicated on ice using Branson digital sonifier (20% output, 15 sec per pulse for 24 times) to obtain an average DNA fragment size of 500 bp. The lysates were centrifuged, and supernatant was collected as soluble chromatin. A twenty-fifth of the total chromatin was collected as input, and the remaining was incubated with anti-HA-agarose beads (A2095; Sigma) at 4° overnight. Beads were collected by centrifugation and washed at room temperature with the following sequence of buffers: twice with FA buffer for 5 min, twice with FA buffer with 500 mM NaCl for 5 min, twice with radioimmunoprecipitation assay buffer (RIPA) buffer (10 mM Tris-HCl at pH 8.0, 250 mM LiCl, 0.5% NP-40, 0.5% Na-deoxycholate, 1 mM EDTA) for 5 min, and twice with 1 × TE for 5 min. Immunoprecipitated DNA was eluted in elution buffer (25 mM Tris-HCl at pH 7.5, 10 mM EDTA, 0.5% SDS) at 65° overnight and the immunoprecipitated samples were treated with proteinase K at 55° for 4 hr. Input samples were mixed with stop buffer (20 mM Tris-HCl at pH 8.0, 100 mM NaCl, 20 mM EDTA, 1% SDS), incubated at 65° overnight, and treated with RNase A at 37° for 2hr and proteinase K at 55° for 2 hr. DNA was extracted once with phenol/chloroform, followed by chloroform, and precipitated with ethanol. Quantitative PCR (qPCR) was performed using 7500 Fast Real Time PCR System with Fast SYBR Green Master Mix (Applied Biosystems), using the following conditions: 95° for 20 sec followed by 40 cycles of 95° for 3 sec, and 60° for 30 sec. Primers used for this study are listed in Table S3.

Sequencing libraries, with two biological replicates from each strain (both input and IP), were prepared using Illumina Nextera DNA Library Kit #FC-121-1031 and 75-base paired-end reads were obtained by multiplexing on a single Illumina NextSeq model 500 run. Reads were aligned to the sacCer3 genome assembly using Bowtie version 1.0.0 with the following parameters: -n2 -3 40 -m3–best–strata -S, and loci of

enrichment were called with input sequences as control using MACS version 2.1.1.20160226 in paired-end mode with the following settings: -g 1.21e7–keep-dup auto -B–SPMR. Pile-ups were generated during peak calling. For enrichment analysis, only peaks common to each replicate were considered. Statistics were performed using Prism 8.

Data availability

Strains and plasmids are available upon request. Sequencing data generated for this study has been deposited in the Gene Expression Omnibus (https://www.ncbi.nlm.nih.gov/geo) under accession number GSE145602. The authors affirm that all data necessary for confirming the conclusions of the article are present within the article, figures, and tables. Supplemental material available at figshare: https://doi.org/10.25386/genetics.11899908.

Results

Cse4 K215/216 at the C terminus are targets for sumoylation

Since Cse4 K215 and K216 (214-M**KK**D-217) meet the criterion for potential SUMO consensus site (GPS-SUMO (Ren *et al.* 2009; Zhao *et al.* 2014; http://sumosp.biocuckoo.org), we examined if Cse4 K215/216 are targets of sumoylation *in vivo*. We mutated both K215 and K216 to arginine (R) and performed an affinity pull-down assay to examine the sumoylation status of transiently overexpressed *GAL-HA-cse4 K215/216R* (K215/216 mutated to R215/216). Pull-down experiments were done using Ni-NTA agarose beads and SUMO-modified species were detected by Western blot analysis with anti-Smt3 antibody (Figure 1A). Strains expressing *HA-CSE4* and *HA-cse4 16KR* (all 16K mutated to R) were used as controls. As described previously (Ohkuni *et al.* 2016; Ohkuni *et al.* 2018), at least three high-molecular-weight sumoylated Cse4 species were observed in wild-type cells (Figure 1A, denoted by arrows) and these SUMO-modified species were not detected in strains expressing vector alone or *HA-cse4 16KR*. Strains expressing *HA-cse4 K215/216R* showed reduced levels of sumoylated Cse4 even though similar levels of Cse4 and Cse4 K215/216R were pulled down (Figure 1A). Quantification showed significant reduction in sumoylation status of Cse4 K215/216R when compared to wild-type Cse4 (Figure 1B). These results suggest that Cse4 K215/216 in the C terminus are the target of sumoylation.

We have recently shown that Cse4 K65 in the N terminus contributes to sumoylation of Cse4 and *cse4 K65R* strains exhibit reduced levels of sumoylation and ubiquitination with defects in proteolysis of Cse4 K65R (Ohkuni *et al.* 2018). The reduced levels of sumoylated Cse4 K215/216R prompted us to examine whether Cse4 K215/216 sumoylation regulates Cse4 proteolysis *in vivo*. Since arginine is also target of methylation, we generated a mutant in which Cse4 K215/216 are changed to alanine (A). Previous studies aimed at defining the role of ubiquitination of Cse4 in Psh1-mediated proteolysis have also used K-to-A substitution (Hewawasam *et al.* 2010). Protein stability assays were performed using whole-cell extracts from cells that transiently overexpressed either *CSE4*, *cse4 K215/216R*, or *cse4 K215/216A* after treatment with CHX to inhibit protein synthesis. Western blot analysis was used to measure levels of HA-Cse4 after CHX treatment. HA-Cse4 was rapidly degraded ($t_{1/2}$ = 34.4 ± 6.9 min) in wild-type strains (Figure 1C), as reported previously (Ohkuni *et al.* 2016). The stability of both HA-Cse4 K215/216R ($t_{1/2}$ = 28.8 ± 3.6 min) and HA-Cse4 K215/216A ($t_{1/2}$ = 27.4 ± 1.6 min) were not significantly different when compared to wild-type HA-Cse4 (Figure 1, C–E). These observations suggest that defects in sumoylation of Cse4 K215/216R do not affect Cse4 proteolysis.

Overexpression of cse4 K215/216R/A does not exhibit SDL in a psh1Δ strain

Previous studies showed that defects in Cse4 proteolysis in a *psh1*Δ strain contribute to its mislocalization to noncentromeric regions and SDL when Cse4 is overexpressed (Hewawasam *et al.* 2010; Ranjitkar *et al.* 2010; Au *et al.* 2013). We examined the growth phenotype of *psh1*Δ strains with *GAL-CSE4*, *GAL-cse4 K215/216R*, or *GAL-cse4 K215/216A*. As expected, the SDL phenotype was observed in a *psh1*Δ strain with *GAL-CSE4* on galactose medium (Figure 2, A and B); however, SDL was not observed in *psh1*Δ strains expressing *GAL-cse4 K215/216R* (Figure 2A) or *GAL-cse4 K215/216A* (Figure 2B). Notably, the growth of the *psh1*Δ strain was better with *GAL-cse4 K215/216A* when compared to *GAL-cse4 K215/216R*. We also examined the proteolysis of Cse4 K215/216R/A in a *psh1*Δ strain. The stability of HA-Cse4 K215/216R and HA-Cse4 K215/216A were not increased when compared to HA-Cse4 in the *psh1*Δ strain (Figure 2, C and D and Figure S1). We conclude that overexpression of *cse4 K215/216R/A* does not lead to SDL or increase the stability of HA-Cse4 K215/216R/A in a *psh1*Δ strain, suggesting that K215/216 sumoylation does not affect Cse4 proteolysis.

Sumoylation of Cse4 K215/216 affects its interaction with Cac2, a subunit of the CAF-1 complex

Similar to our finding that overexpression of *cse4 K215/216R/A* suppresses the SDL in a *psh1*Δ strain, Hewawasam *et al.* showed that deletion of *CAC2*, which encodes one of the subunits of the CAF-1 complex, suppresses the SDL phenotype of *GAL-CSE4* in a *psh1*Δ strain (Hewawasam *et al.* 2018). Furthermore, these authors showed that the CAF-1 complex interacts with Cse4 and regulates deposition of overexpressed Cse4 into noncentromeric chromatin (Hewawasam *et al.* 2018).

We hypothesized that sumoylation of Cse4 K215/216 may regulate its interaction with Cac2, facilitating deposition of overexpressed Cse4 into noncentromeric regions, which in turn contributes to the SDL phenotype of *GAL-CSE4* in a *psh1*Δ strain. To examine this, we performed Co-IP experiments with strains coexpressing either *HA-CSE4* or *HA-cse4 K215/216R/A* with *CAC2-FLAG* (Figure 3). Consistent with previous results (Hewawasam *et al.* 2018), immunoprecipitation with anti-FLAG showed an interaction between Cac2 and Cse4, but not the control lacking Cac2-FLAG (Figure 3A). In

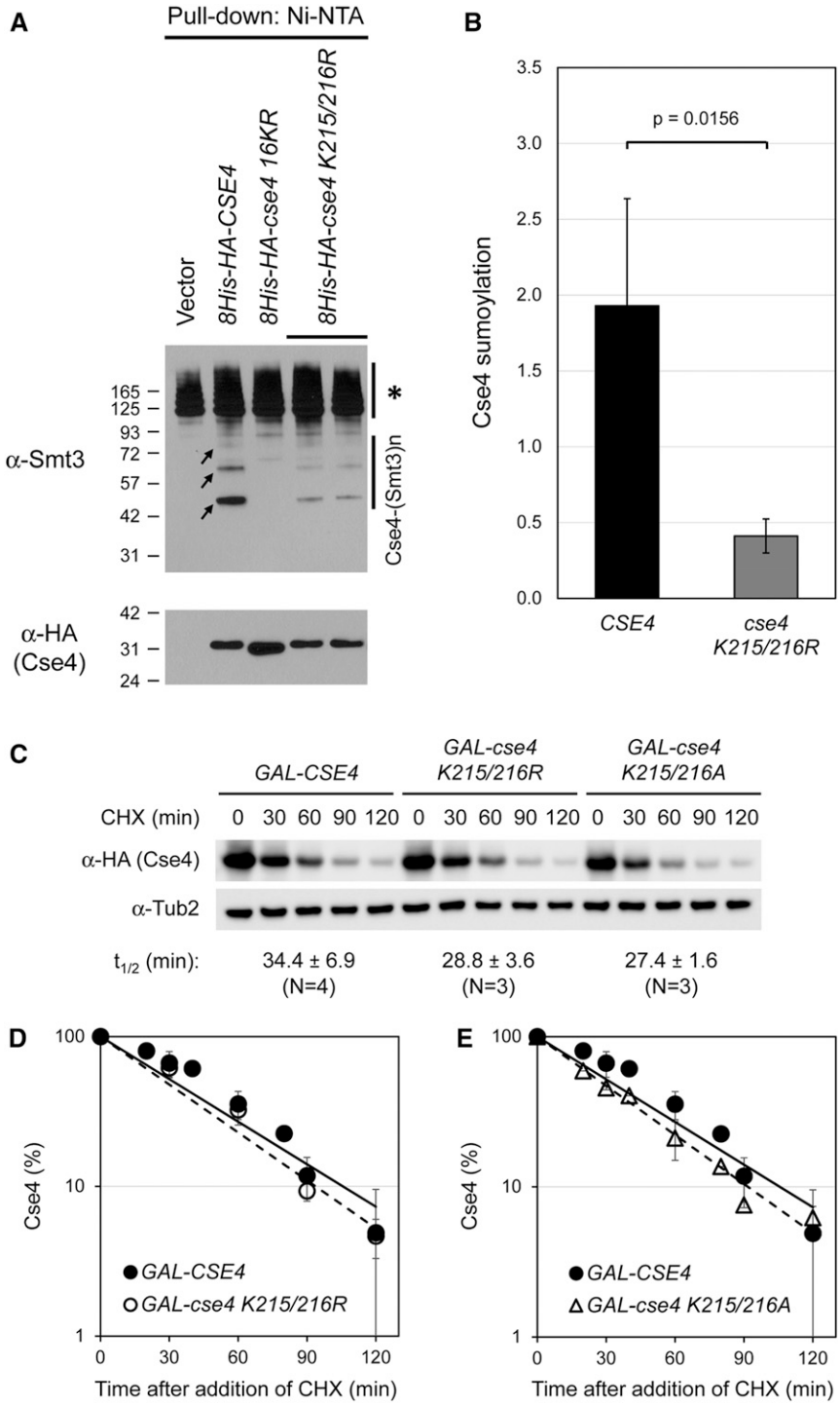

Figure 1 Lysines 215 and 216 are targets of Cse4 sumoylation. (A) Cell lysates were prepared from a wild-type strain (BY4741) transformed with vector (pYES2), *pGAL-8His-HA-CSE4* (pMB1345), *pGAL-8His-HA-cse4 16KR* (pMB1344), or *pGAL-8His-HA-cse4 K215/216R* (pMB1768). Sumoylation of 8His-HA-Cse4 and nonmodified 8His-HA-Cse4 were detected using cell lysates after pull down on Ni-NTA beads, followed by Western blot analysis with anti-Smt3 and anti-HA (Cse4) antibodies, respectively. At least three high-molecular-weight bands of 8His-HA-Cse4 (arrows) were detected. Asterisk shows nonspecific sumoylated proteins that bind to beads. (B) Relative sumoylation of Cse4 in arbitrary density units (normalized to nonmodified Cse4 probed by anti-HA in pull-down sample) determined in multiple experiments (*CSE4*: $N = 4$, *cse4 K215/216R*: $N = 3$). Statistical significance was assessed by unpaired *t*-test. Error bars indicate SD from the mean. (C) *cse4 K215/216R/A* mutants do not exhibit defects in Cse4 proteolysis. A wild-type (BY4741) strain transformed with either *pGAL-6His-3HA-CSE4* (pMB1458), *pGAL-6His-3HA-cse4 K215/216R* (pMB1789), or *pGAL-6His-3HA-cse4 K215/216A* (pMB1675) were grown in galactose (2%) medium for 2 hr. Glucose (2%) containing cycloheximide (CHX; 10 μg/ml) was added and cells were collected at the indicated time points. Blots were probed with anti-HA (Cse4) or anti-Tub2 (loading control) antibody. Cse4 protein half-life ($t_{1/2}$) represents the mean of multiple biological repeats with SD. The difference in $t_{1/2}$ is not statistically significant (*P*-values: *CSE4 vs. cse4 K215/216R*, 0.3630; *CSE4 vs. cse4 K215/216A*, 0.2316). (D) Kinetics of turnover in Cse4 K215/216R from C. The graph shows the percentage of Cse4 signals normalized to Tub2 at the indicated time points. (E) Kinetics of turnover in Cse4 K215/216A from C.

contrast, significantly reduced interaction was observed between Cac2 and Cse4 K215/216R or Cse4 K215/216A (Figure 3, A and B), leading us to propose that sumoylation of Cse4 K215/216 contributes to its interaction with the CAF-1 subunit Cac2.

Sumoylation of Cse4 K215/216 regulates its enrichment in chromatin and localization to noncentromeric regions

Given the reduced interaction of Cac2 with Cse4 K215/216R/A, we reasoned that levels of chromatin-associated Cse4 K215/216R/A would also be reduced. We performed subcellular fractionation to examine the levels of Cse4 and Cse4 K215/216R/A in soluble and chromatin fractions (Figure 4, A and B and Figure S2). Pgk1 and histone H3 served as controls for the soluble and the chromatin fractions, respectively. Consistent with our hypothesis, levels of chromatin-associated Cse4 K215/216R and Cse4 K215/216A are significantly reduced as compared to wild-type Cse4 (Figure 4, A and B and Figure S2). In contrast, levels of Cse4 K215/216R and

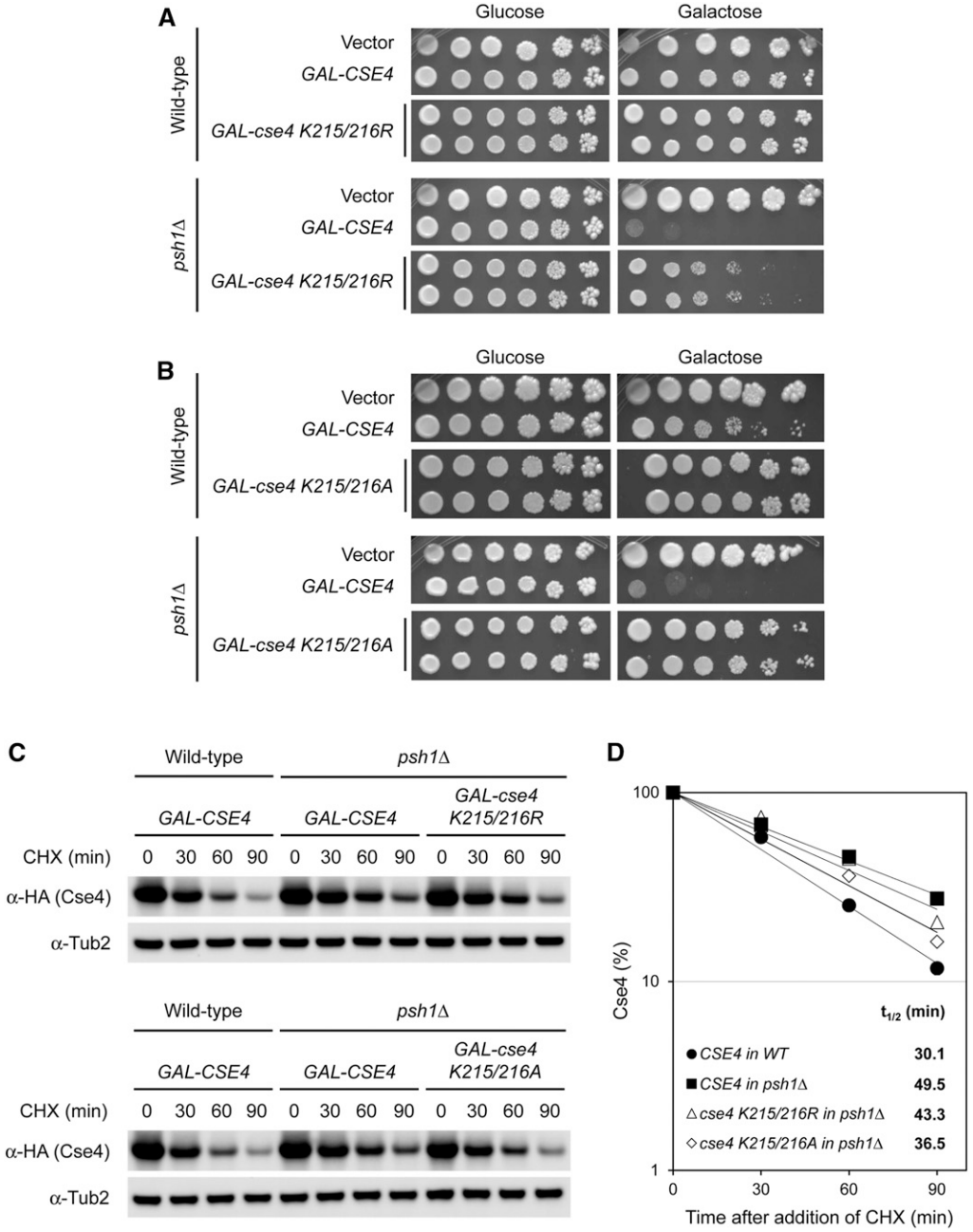

Figure 2 Overexpression of *cse4 K215/216R/A* does not exhibit Synthetic Dosage Lethality (SDL) in a *psh1*Δ strain. (A and B) Overexpression of *cse4 K215/216R/A* does not result in SDL in a *psh1*Δ strain. Fivefold serial dilutions of the indicated strains were plated on glucose (2%)- or galactose (2%)-containing synthetic medium selective for the plasmid. The plates were incubated at 30° for 4 days and photographed. Wild-type (BY4741) and *psh1*Δ (YMB9034) cells transformed with vector (pYES2), *pGAL-8His-HA-CSE4* (pMB1345), or *pGAL-8His-HA-cse4 K215/216R* (pMB1768) were used in A. Wild-type (BY4741) and *psh1*Δ (YMB9034) cells transformed with vector (pMB433), *pGAL-6His-3HA-CSE4* (pMB1458), or *pGAL-6His-3HA-cse4 K215/216A* (pMB1675) were used in B. (C) The stability of HA-Cse4 K215/216R/A is not increased when compared to HA-Cse4 in a *psh1*Δ strain. Wild-type (BY4741) and *psh1*Δ (YMB9034) strains transformed with either *pGAL-6His-3HA-CSE4* (pMB1458), *pGAL-6His-3HA-cse4 K215/216R* (pMB1789), or *pGAL-6His-3HA-cse4 K215/216A* (pMB1675) were assayed as described in Figure 1C. (D) Kinetics of turnover from C. Cse4 protein half-life ($t_{1/2}$) is indicated. Error bars of *CSE4* in wild type (WT) and *CSE4* in *psh1*Δ represent average deviation of two replicates.

Cse4 K215/216A in the soluble fraction were similar to that of Cse4, implying that sumoylation of Cse4 K215/216 facilitates its deposition into chromatin.

Based on our results showing reduced enrichment of Cse4 K215/216R/A in the chromatin fraction, we hypothesized that Cse4 K215/216 sumoylation facilitates deposition of overexpressed Cse4 into noncentromeric chromatin. Previous studies have shown high levels of overexpressed Cse4 at promoters of *PHO5*, *SLP1*, *SAP4*, and *RDS1* in a *psh1*Δ strain, but not in a wild-type strain (Hildebrand and Biggins 2016; Hewawasam *et al.* 2018). We performed chromatin immunoprecipitation (ChIP)/qPCR experiments in a *psh1*Δ strain to examine the localization of Cse4 K215/216R/A at the promoters of *PHO5*, *SLP1*, *SAP4*, and *RDS1*. As expected, an enrichment of Cse4 was observed at the promoters of these genes in a *psh1*Δ strain; however, significantly reduced levels of Cse4 K215/216R/A were observed at the promoters of these genes as compared to wild-type Cse4 (Figure 4, C–F). The reduced enrichment of Cse4 K215/216R/A in chromatin and localization to noncentromeric regions are consistent with defects in the interaction of Cse4 K215/216R/A with Cac2. These results suggest that sumoylation of Cse4 K215/216 promotes its mislocalization to noncentromeric regions.

To further analyze the contribution of Cse4 K215/216 sumoylation to its genome-wide localization, we performed

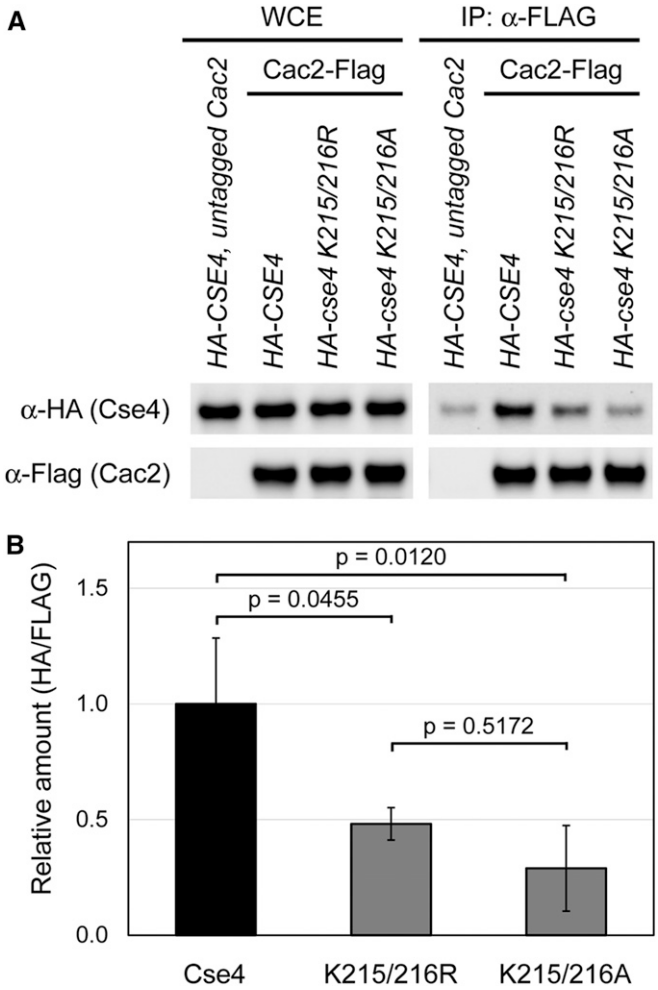

Figure 3 Cse4 K215/216 are required for efficient interaction of Cse4 with the CAF-1 subunit Cac2. (A) Cse4 K215/216R/A shows reduced interaction with Cac2. Co-IP experiments were performed using protein extracts, prepared from the indicated strains, with anti-FLAG agarose antibody. Samples were resolved by SDS-PAGE and levels of Cse4 and Cac2 were detected by Western blot analysis with anti-HA and anti-FLAG antibodies, respectively. Isogenic yeast strains were as follows: Cac2-Flag (YMB10975) transformed with either *pGAL-6His-3HA-CSE4* (pMB1458), *pGAL-6His-3HA-cse4 K215/216R* (pMB1789), or *pGAL-6His-3HA-cse4 K215/216A* (pMB1675); and untagged Cac2 (BY4741) transformed with *pGAL-6His-3HA-CSE4* (pMB1458) for negative control. WCE, whole-cell extract. (B) Levels of Cse4 (α-HA, IP) after immunoprecipitation of Cac2-FLAG were quantified after normalization to Cac2 levels in the IP (α-FLAG, IP) in three independent experiments. Statistical significance of the normalized values was assessed by one-way ANOVA ($P = 0.0125$) followed by Tukey post test (all pairwise comparisons of means). Error bars show SD from the mean.

ChIP-sequencing experiments to examine the localization of overexpressed Cse4 or Cse4 K215/216R/A in a *psh1*Δ strain. The results showed that genome-wide enrichment of both Cse4 K215/216R and Cse4 K215/216A were reduced when compared to wild-type Cse4 (Figure 5A). For validation, we performed qPCR focusing on a subset of noncentromeric regions. Our results showed reduced enrichment of Cse4 K215/216R and Cse4 K215/216A when compared to wild-type Cse4 at intergenic regions such as *UGA3/UGX2* convergent region (Figure 5B), *FIG4/LEM3* divergent promoter (Figure 5C), and *COQ3* promoter (Figure 5D) and the coding region of *GUP2* (Figure 5E), suggesting that sumoylation of Cse4 K215/216 facilitates mislocalization of overexpressed Cse4 to noncentromeric regions genome-wide.

Sumoylation of Cse4 K215/216 affects its association with the Cse4 chaperone Scm3 and centromeric chromatin

We next examined the effects of Cse4 K215/216R/A mutations on the localization of Cse4 to centromeric chromatin. ChIP/qPCR experiments showed reduced levels of Cse4 K215/216R and Cse4 K215/216A at *CEN1* and *CEN3* regions (Figure 6, A and B). The chaperone Scm3 (HJURP in humans) is responsible for centromeric localization of Cse4 (Camahort *et al.* 2007; Mizuguchi *et al.* 2007; Stoler *et al.* 2007). The reduced centromeric localization of Cse4 K215/216R and Cse4 K215/216A prompted us to examine if the interaction with Scm3 is also reduced. We performed Co-IP experiments using strains coexpressing either *HA-CSE4* or *HA-cse4 K215/216R/A* with *SCM3-FLAG* (Figure 6, C and D). As expected, immunoprecipitation with anti-FLAG showed an interaction between Scm3 and Cse4, but not the control lacking Scm3-FLAG. Consistent with our hypothesis, significantly reduced interaction was observed between Scm3 and Cse4 K215/216R and Cse4 K215/216A (Figure 6, C and D).

SCM3 is essential for haploid growth; however, overexpression of *CSE4* can rescue the lethality of strains depleted for Scm3 (Scm3^{off}) (Camahort *et al.* 2009). Since overexpressed Cse4 is unable to rescue the growth of Scm3^{off} strains when *CAC2* is deleted, CAF-1 is proposed to be the primary chaperone targeting overexpressed Cse4 to the centromeres when Scm3 is depleted (Hewawasam *et al.* 2018). Given the reduced interaction of Cse4 K215/216R/A with Cac2 (Figure 3), we hypothesized that the lethality of Scm3^{off} strains may not be rescued by overexpression of *cse4 K215/216R/A*. Growth assays were performed using a strain in which expression of *SCM3* is regulated by the *GAL* promoter and expression of *CSE4* or *cse4 K215/216R* regulated by a copper-inducible promoter on a plasmid. The Scm3^{on} strain is viable on galactose medium with or without copper (Figure 6E). The Scm3^{off} strain is viable on glucose medium only when *CSE4* is overexpressed on copper-containing medium (Figure 6E, row 5), but not when *cse4 K215/216R* was similarly overexpressed (Figure 6E, row 6). The lack of complete suppression of growth in strains expressing copper-inducible *cse4 K215/216R* are not due to reduced levels of Cse4 K215/216R compared to Cse4 (Figure S3). Taken together, we propose that sumoylation of overexpressed Cse4 K215/216 promotes its association with centromeric chromatin (via CAF-1) when Scm3 is depleted.

Our results so far have shown reduced deposition of overexpressed Cse4 into both centromeric and noncentromeric chromatin in the absence of K215/216 sumoylation, prompting us to ask if Cse4 215/216R/A mutation might lead to defects in chromosome segregation under normal

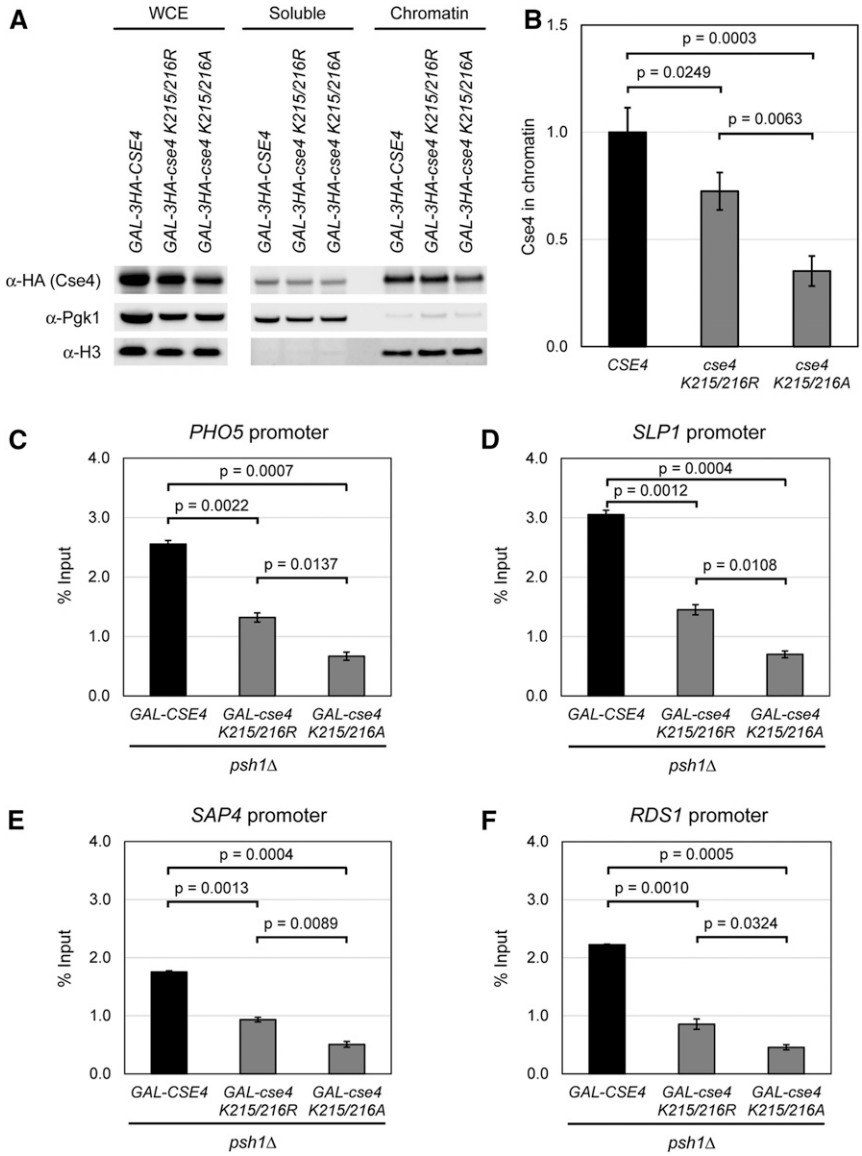

Figure 4 Cse4 K215/216 regulates its enrichment in chromatin and localization to noncentromeric regions. (A) Levels of chromatin-associated Cse4 K215/216R/A are reduced when compared to wild-type Cse4. Subcellular fractionation experiments were done using a wild-type (BY4741) strain transformed with *pGAL-3HA-CSE4* (pMB1597), *pGAL-3HA-cse4 K215/216R* (pMB1815), or *pGAL-3HA-cse4 K215/216A* (pMB1677). Whole-cell extracts (WCEs) were fractionated into soluble and chromatin fractions. Cse4 levels in each fraction were monitored by Western blot analysis with anti-HA antibody. Pgk1 and histone H3 were used as markers for soluble and chromatin fractions, respectively. (B) Levels of chromatin bound Cse4 were quantified after normalization to H3 levels in the chromatin in three independent experiments. Statistical significance of the normalized values was assessed by one-way ANOVA (P = 0.0004) followed by Tukey post test (all pairwise comparisons of means). Error bars show SD from the mean. (C–F) Reduced levels of Cse4 K215/216R/A at noncentromeric regions. ChIP-qPCR experiments were done using chromatin prepared from *psh1*Δ (YMB9034) strain transformed with *pGAL-6His-3HA-CSE4* (pMB1458), *pGAL-6His-3HA-cse4 K215/216R* (pMB1789), or *pGAL-6His-3HA-cse4 K215/216A* (pMB1675), and assayed for association with (C) *PHO5*, (D) *SLP1*, (E) *SAP4*, and (F) *RDS1* promoter regions. Statistical significance was assessed by one-way ANOVA (P = 0.0007, *PHO5*; P = 0.0004, *SLP1*; P = 0.0004, *SAP4*; P = 0.0004, *RDS1*) followed by Tukey post test (all pairwise comparisons of means). Error bars show average deviation of two biological repeats.

physiological conditions. We tested the effect of Cse4 K215/216R/A mutations on chromosome segregation using a colony sectoring assay that measures the frequency of loss of a nonessential RC resulting in red sectors in an otherwise white colony. Our results showed that strains expressing *cse4 K215/216R* and *cse4 K215/216A* from their endogenous promoter showed 2.5- to 4-fold higher loss of the RC when compared to that observed in a wild-type strain (Figure 6F).

Biological role of Cse4 K215/216 sumoylation is independent of the role of Cse4 K65 sumoylation

We have previously shown that N-terminal sumoylation of Cse4 K65 regulates Cse4 proteolysis and prevents mislocalization to noncentromeric regions (Ohkuni *et al.* 2018). To examine the biological relationship between sumoylation at Cse4 K65 and at K215/216, we constructed a strain expressing *cse4 K65/215/216R* and tested it for sumoylation, ability to suppress *GAL-CSE4* SDL in a *psh1*Δ strain, interaction with Cac2 and Scm3, and chromosomal association with centromeric and noncentromeric regions. The sumoylation status of Cse4 and Cse4 mutants (K65R, K215/216R, K65/215/216R) was assayed using whole-cell extracts (Figure 7, A and B). As expected, Cse4 K65R and Cse4 K215/216R showed significant reduction in sumoylation when compared to Cse4 (Figure 7B). Furthermore, sumoylation of Cse4 K65R was not significantly different from that of Cse4 K215/216R (Figure 7B). The sumoylation of Cse4 K65/215/216R was significantly reduced when compared to that observed either Cse4 K65R or Cse4 K215/216R (Figure 7B). In agreement with our previous studies (Ohkuni *et al.* 2016), we failed to detect SUMO-modified Cse4 species in the *siz1*Δ *siz2*Δ (deletion of SUMO E3 ligases) strain (Figure 7A). Hence, we conclude that both K65 and K215/216 are targets of Cse4 sumoylation.

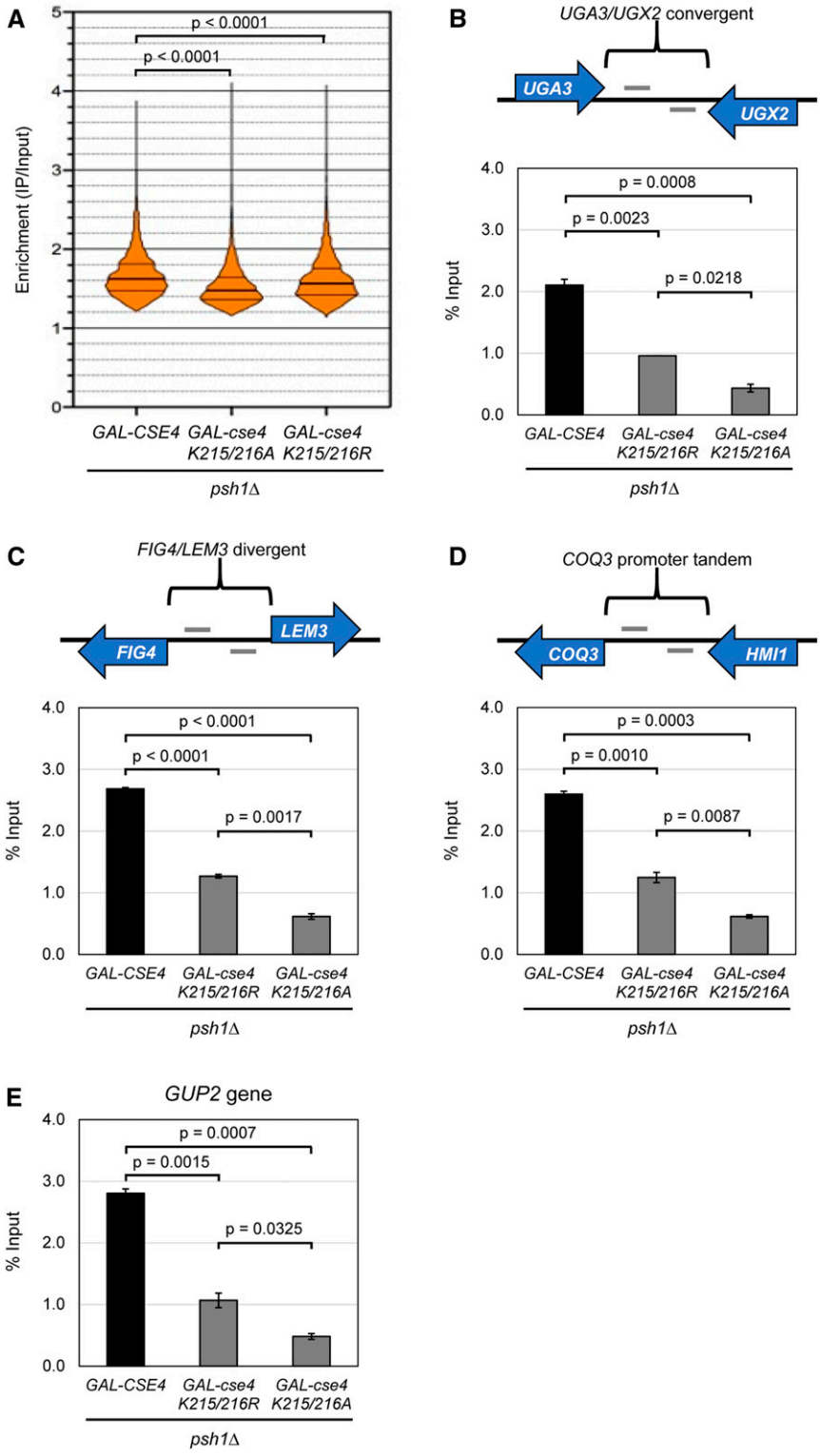

Figure 5 Cse4 K215/216 regulates genome-wide mislocalization of Cse4 to non-*CEN* regions. ChIP was performed using chromatin prepared from *psh1*Δ (YMB9034) strain transformed with *pGAL-6His-3HA-CSE4* (pMB1458), *pGAL-6His-3HA-cse4 K215/216R* (pMB1789), or *pGAL-6His-3HA-cse4 K215/216A* (pMB1675). Input and IP samples were used for ChIP-sequencing as described in *Materials and Methods*. (A) The violin plot shows Cse4 genome-wide enrichment for *GAL-CSE4*, *GAL-cse4 K215/216R*, and *GAL-cse4 K215/216A* in a *psh1*Δ background. Mean Cse4 enrichment for both K215/216 mutants was significantly less than that of wild type ($P < 0.0001$ by one-way ANOVA with Dunnett's post test). (B–E) For validation of the ChIP-sequencing, qPCR was performed to assay association of Cse4 levels at intergenic regions and a coding region of a gene. (B) *UGA3*/*UGX2* convergent, (C) FIG4/*LEM3* divergent, (D) *COQ3* tandem, and (E) open reading frame of *GUP2* were tested. Statistical significance was assessed by one-way ANOVA ($P = 0.0008$, *UGA3*/*UGX2*; $P < 0.0001$, FIG4/*LEM3*; $P = 0.0003$, *COQ3*; $P = 0.0006$, *GUP2*) followed by Tukey post test (all pairwise comparisons of means). Error bars show average deviation of two biological repeats. Gray line in B-D represents position of the primer set.

We next used the *cse4 K65R*, *cse4 K215/216R*, and *cse4 K65/215/216R* strains to examine the functional relationship between Cse4 K65 and Cse4 K215/216 sumoylation. In the first approach, we examined the ability of *GAL-cse4 K65/215/216R* to suppress SDL in a *psh1*Δ strain. As expected, *GAL-CSE4* and *GAL-cse4 K65R* exhibit SDL phenotype in *psh1*Δ strains on galactose medium (Figure 7C). As shown earlier (Figure 2A), *GAL-cse4 K215/216R* did not lead to SDL in a *psh1*Δ strain (Figure 7C). The triple mutant expressing *GAL-cse4 K65/215/216R* also did not show SDL in a *psh1*Δ strain (Figure 7C). *slx5*Δ

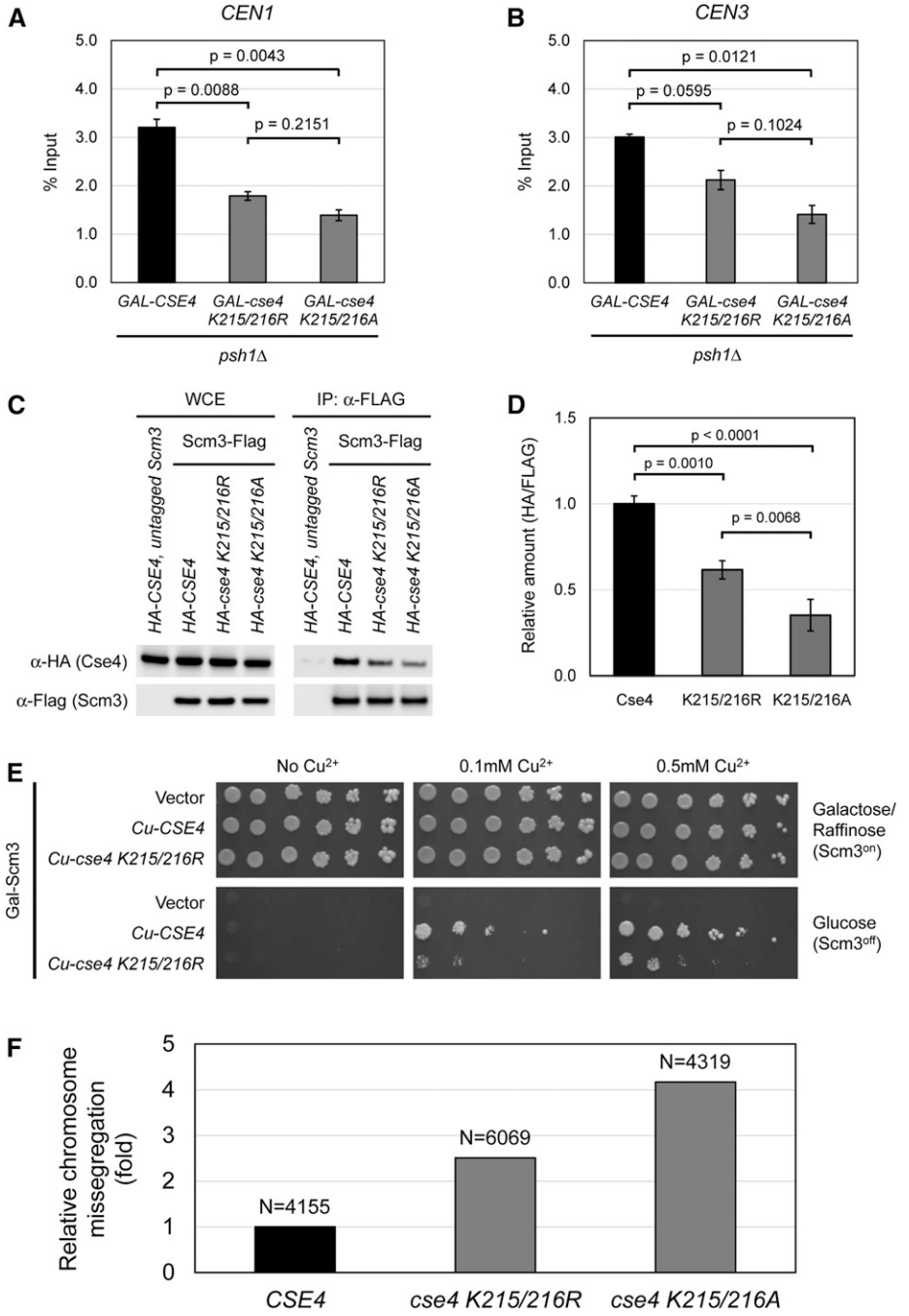

Figure 6 Cse4 K215/216 regulates localization of Cse4 to *CEN* regions and interaction with Scm3. (A and B) ChIP-qPCR experiments were done using chromatin prepared from a *psh1*Δ (YMB9034) strain transformed with *pGAL-6His-3HA-CSE4* (pMB1458), *pGAL-6His-3HA-cse4 K215/216R* (pMB1789), or *pGAL-6His-3HA-cse4 K215/216A* (pMB1675). The association at (A) *CEN1* and (B) *CEN3* were assayed. Statistical significance was assessed by one-way ANOVA ($P = 0.0042$, *CEN1*; $P = 0.0136$, *CEN3*) followed by Tukey post test (all pairwise comparisons of means). Error bars show the average deviation of two biological repeats. (C) Cse4 K215/216R/A shows reduced interaction with Scm3. Co-IP experiments were performed using protein extracts, prepared from the indicated strains, with anti-FLAG agarose antibody. Samples were resolved by SDS-PAGE and levels of Cse4 and Scm3 were detected by Western blot analysis with anti-HA and anti-FLAG antibodies, respectively. Isogenic yeast strains were as follows: Scm3-Flag (YMB10976) transformed with either *pGAL-6His-3HA-CSE4* (pMB1458), *pGAL-6His-3HA-cse4 K215/216R* (pMB1789), or *pGAL-6His-3HA-cse4 K215/216A* (pMB1675); and untagged Scm3 (BY4741) transformed with *pGAL-6His-3HA-CSE4* (pMB1458) for negative control. WCE, whole-cell extract. (D) Levels of Cse4 (α-HA, IP) after immunoprecipitation of Scm3-FLAG were quantified after normalization to Scm3 levels in the IP (α-FLAG, IP) in three biological repeats. Statistical significance of the normalized values was assessed by one-way ANOVA ($P < 0.0001$) followed by Tukey post test (all pairwise comparisons of means). Error bars show SD from the mean. (E) Overexpression of *cse4 K215/216R* fails to rescue the growth of Scm3^{off} strain. Scm3 expression under the *GAL* promoter was controlled by addition of galactose (Scm3^{on}) and glucose (Scm3^{off}). *CSE4* overexpression was controlled by a copper-inducible promoter on a plasmid. Overexpression of *CSE4* (0.5 mM copper) can rescue the growth of Scm3^{off} strains on glucose media due to chaperone activity of CAF-1 to assemble to Cse4 at centromeres. Overexpression of *cse4 K215/216R* (0.5 mM copper) does not rescue the growth defect of Scm3^{off} strain on glucose medium. Cells were spotted in fivefold dilutions on the plates indicated, incubated at 30° for 3 days, and photographed. Isogenic yeast strains are *GAL-SCM3* transformed with vector (JG1689), *Cu-CSE4* (JG1690), or *Cu-cse4 K215/216R* (YMB11165). (F) *cse4 K215/216R/A* mutants exhibit increased chromosome loss under normal physiological condition. Yeast strains (*CSE4*: YMB10298, *cse4 K215/216R*: YMB10300, *cse4 K215/216A*: YMB10299) were plated on SD with limiting adenine and incubated for 5 days at 30°. Chromosome loss was determined by counting the number of colonies that exhibit sectoring phenotype due to loss of nonessential RC. The number of sectored colonies/total colonies from three independent clones were *CSE4*: 3/4155, *cse4 K215/216R*: 11/6069, and *cse4 K215/216A*: 13/4319. Graph shows chromosome loss relative to that observed in the *CSE4* strain normalized to 1.0.

and *hir2*Δ strains, which are defective in Cse4 proteolysis, similarly exhibit SDL with *GAL-CSE4* (Ohkuni *et al.* 2016; Ciftci-Yilmaz *et al.* 2018). We examined the ability of *GAL-cse4 K65/215/216R* to suppress SDL in these strains as well. The results showed that *slx5*Δ and *hir2*Δ strains expressing *GAL-CSE4* or *GAL-cse4 K65R* exhibit SDL on galactose medium (Figure S4), although the growth inhibition was not as pronounced as that observed with the *psh1*Δ strain expressing *GAL-CSE4* or *GAL-cse4 K65R* (Figure 7C). This is not surprising since Slx5 regulates Psh1-independent proteolysis of Cse4, and Hir2 regulates Psh1 and other pathways for proteolysis of Cse4 (Ohkuni *et al.* 2016; Ciftci-Yilmaz *et al.* 2018). The *slx5*Δ and *hir2*Δ

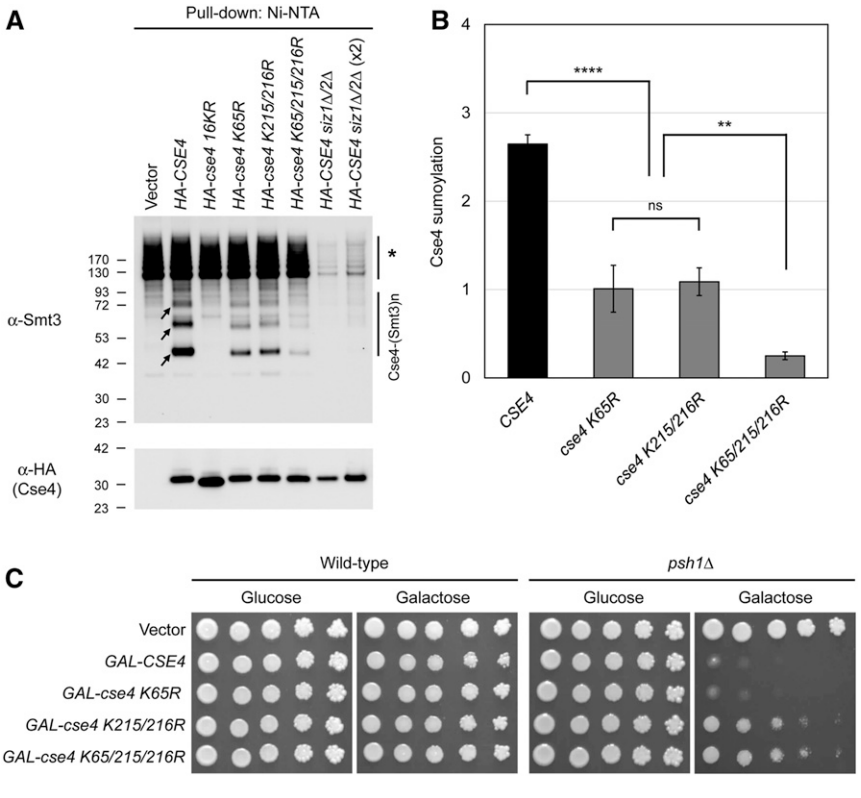

Figure 7 Cse4 K65 and Cse4 K215/216 contribute to sumoylation of Cse4 and the SDL of *GAL-cse4 K65R* in *psh1*Δ is suppressed by *cse4 K215/216R*. (A) Cse4 K65 and Cse4 K215/216 contribute to sumoylation of Cse4. Wild-type strain (BY4741) transformed with vector (pYES2), *pGAL-8His-HA-CSE4* (pMB1345), *pGAL-8His-HA-cse4 16KR* (pMB1344), *pGAL-8His-HA-cse4 K65R* (pMB1762), *pGAL-8His-HA-cse4 K215/216R* (pMB1768), or *pGAL-8His-HA-cse4 K65/215/216R* (pMB1769) were assayed as described in Figure 1A. Cse4 sumoylated species (arrows) and nonspecific sumoylated species that bind to beads (asterisk) are shown. A *siz1*Δ *siz2*Δ strain (YMB7277) transformed with pMB1345 was used for an additional negative control. Because of the defect in the induction of *GAL-CSE4* in *siz1*Δ *siz2*Δ strain (Ohkuni *et al.* 2016), we used x1 and x2 protein levels of pull-down sample from this strain. (B) Quantification of relative sumoylation of Cse4 and Cse4 mutants (K65R, K215/216R, K65/215/216R) in arbitrary density units (normalized to nonmodified Cse4 probed by anti-HA in pull-down sample) determined in three biological repeats. Statistical significance was assessed by one-way ANOVA ($P < 0.0001$) followed by Tukey post test (all pairwise comparisons of means). Error bars indicate SD from the mean. $^{**}P < 0.01$, $^{****}P < 0.0001$. ns, not significant. (C) *GAL-cse4 K65R* exhibits SDL in a *psh1*Δ strain and this is suppressed by *cse4 K215/216R*. Growth assays were done using fivefold serial dilutions of the indicated strains plated on glucose (2%)- or galactose (2%)-containing synthetic medium selective for the plasmid. The plates were incubated at 30° for 3 days and photographed. Wild-type (BY4741) and *psh1*Δ (YMB9034) cells transformed with vector (pYES2), *pGAL-8His-HA-CSE4* (pMB1345), *pGAL-8His-HA-cse4 K65R* (pMB1762), *pGAL-8His-HA-cse4 K215/216R* (pMB1768), or *pGAL-8His-HA-cse4 K65/215/216R* (pMB1769) were used.

strains expressing *GAL-cse4 K215/216R* or *GAL-cse4 K65/215/216R* do not exhibit SDL phenotype (Figure S4). Taken together, these results show that the SDL of *GAL-cse4 K65R* is suppressed, intra-allelically, by *cse4 K215/216R* in *psh1*Δ, *slx5*Δ, and *hir2*Δ strains; in the presence of *K215/216R*, the *K65R* phenotype is masked.

In the second approach, we examined the interaction of Cse4 and Cse4 mutants (K65R, K215/216R, K65/215/216R) with Cac2 and Scm3. As shown earlier (Figure 3), Co-IP experiments with anti-FLAG showed significantly reduced Cse4 K215/216R-Cac2 interaction when compared to Cse4-Cac2 interaction; however, Cse4 K65R-Cac2 interaction was similar to that observed for Cse4-Cac2 (Figure 8, A and B). The interaction of the triple mutant Cse4 K65/215/216R with Cac2 was not significantly different from that observed for the double mutant Cse4 K215/216R (Figure 8, A and B). The interaction of the triple mutant with Scm3 is shown in Figure 8, C and D. As found earlier, Co-IP with anti-FLAG showed significantly reduced Cse4 K215/216R-Scm3 interaction when compared to wild-type Cse4 (Figure 8, C and D). Although the interaction of Cse4 K65R-Scm3 was reduced compared to Cse4-Scm3, a significant difference for the interaction of Scm3 with either the double Cse4 K215/216R or the triple mutant Cse4 K65/215/216R was not observed (Figure 8, C and D).

In the third approach, we examined the localization of Cse4 and Cse4 mutants (K65R, K215/216R, K65/215/216R) to noncentromeric and centromeric regions using ChIP/qPCR (Figure 8E). As shown earlier, ChIP/qPCR showed significantly reduced localization of Cse4 K215/216R when compared to that for Cse4 to noncentromeric regions (*RDS1* and *FIG4/LEM3* divergent promoter regions and the coding region of *GUP2*) and a centromeric region (*CEN3*) (Figure 8E); however, the localization of Cse4 K65R to these regions was not reduced compared to the localization of Cse4 (Figure 8E). Furthermore, the localization of the triple mutant Cse4 K65/215/216R to noncentromeric regions or *CEN3* was not significantly different from the localization of the double mutant Cse4 K215/216R to these regions (Figure 8E). Taken together, these results show that the phenotypes (SDL, interactions with Cac2 and Scm3, and chromosomal localization) of the triple mutant *cse4 K65/215/216R* are similar to those for the double mutant *cse4 K215/216R*. The overexpression phenotypes of *cse4 K65R* are not observed in the additional presence of *cse4 K215/216R*, presumably because the reduced interaction with Cse4 chaperones Scm3 and Cac2 contributes to reduced deposition into chromatin. Thus, the biological role of Cse4 K215/216 sumoylation is independent of the role of Cse4 K65 sumoylation.

Discussion

We have identified K215/216 as sumoylation sites in the C terminus of Cse4 and present multiple lines of evidence

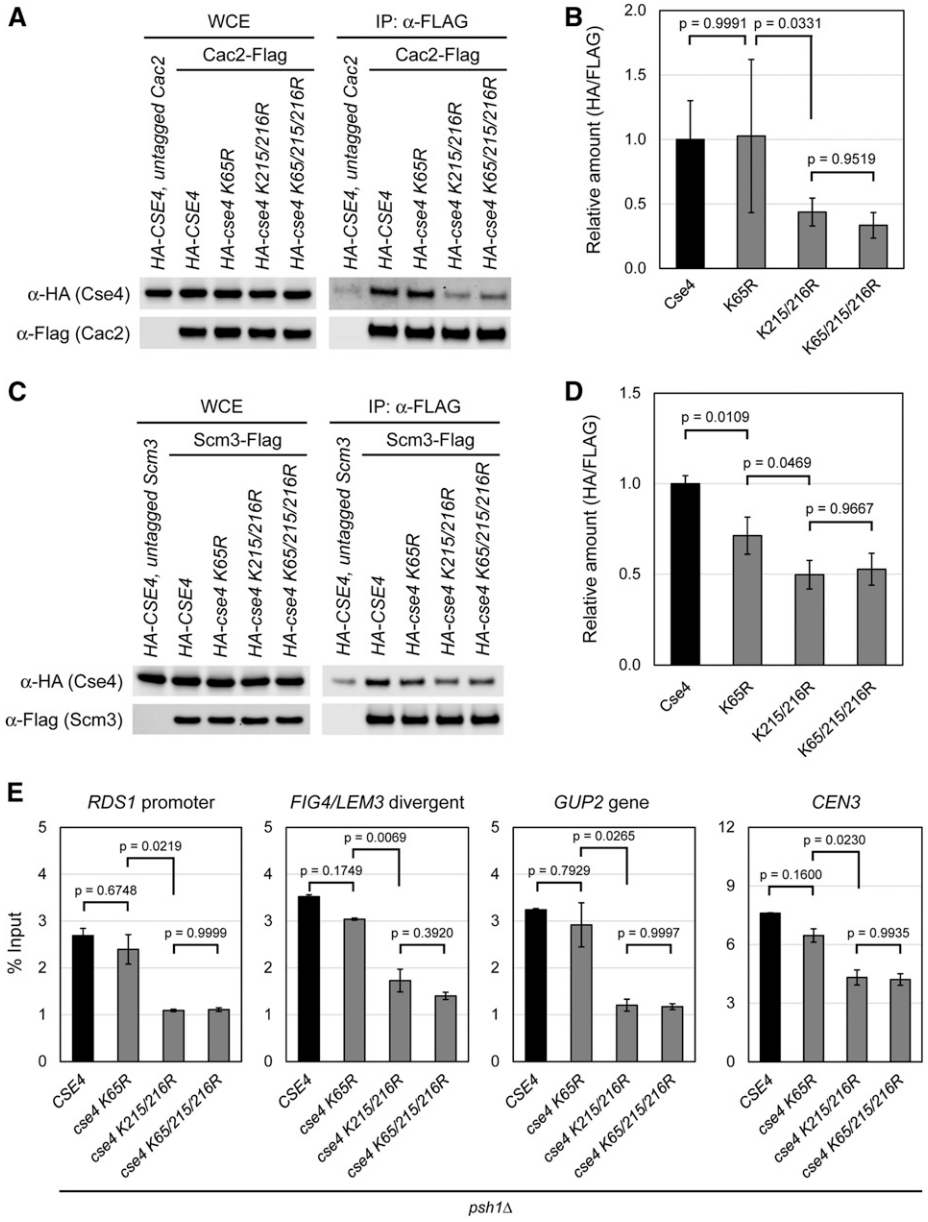

Figure 8 Biological role of Cse4 K215/216 sumoylation is independent of the role of Cse4 K65 sumoylation. (A) The interaction of Cse4 K65/215/216R with Cac2 is similar to that of Cse4 K215/216R with Cac2. Co-IP experiments were performed as described in Figure 3A, using the following strains: Cac2-Flag (YMB10975) transformed with either *pGAL-6His-3HA-CSE4* (pMB1458), *pGAL-6His-3HA-cse4 K65R* (pMB1791), *pGAL-6His-3HA-cse4 K215/216R* (pMB1789), or *pGAL-6His-3HA-cse4 K65/215/216R* (pMB1792). WCE, whole-cell extract. (B) Quantification of interaction of Cse4 and Cse4 mutants (K65R, K215/216R, K65/215/216R) with Cac2. Levels of Cse4 (α-HA, IP) after immunoprecipitation of Cac2-FLAG were quantified after normalization to Cac2 levels in the IP (α-FLAG, IP) from six biological repeats. Statistical significance of the normalized values was assessed by one-way ANOVA ($P = 0.0023$) followed by Tukey post test (all pairwise comparisons of means). Error bars show SD from the mean. (C) The interaction of Cse4 K65/215/216R with Scm3 is similar to that of Cse4 K215/216R with Scm3. Co-IP experiments were performed as described in Figure 6C, using the following strains: Scm3-Flag (YMB10976) transformed with either *pGAL-6His-3HA-CSE4* (pMB1458), *pGAL-6His-3HA-cse4 K65R* (pMB1791), *pGAL-6His-3HA-cse4 K215/216R* (pMB1789), or *pGAL-6His-3HA-cse4 K65/215/216R* (pMB1792). WCE, whole-cell extract. (D) Quantification of interaction of Cse4 and Cse4 mutants (K65R, K215/216R, K65/215/216R) with Scm3. Levels of Cse4 (α-HA, IP) after immunoprecipitation of Scm3-FLAG were quantified after normalization to Scm3 levels in the IP (α-FLAG, IP) from three biological repeats. Statistical significance of the normalized values was assessed by one-way ANOVA ($P = 0.0002$) followed by Tukey post test (all pairwise comparisons of means). Error bars show SD from the mean. (E) The localization of Cse4 K65/215/216R to chromosomal loci is similar to that observed for the localization of Cse4 K215/216R. ChIP-qPCR experiments were done from *psh1*Δ strain (YMB9034) transformed with *pGAL-6His-3HA-CSE4* (pMB1458), *pGAL-6His-3HA-cse4 K65R* (pMB1791), *pGAL-6His-3HA-cse4 K215/216R* (pMB1789), or *pGAL-6His-3HA-cse4 K65/215/216R* (pMB1792), and assayed for association with *RDS1* and FIG4/*LEM3* divergent promoter regions, open reading frame of *GUP2*, and *CEN3*. Statistical significance was assessed by one-way ANOVA ($P = 0.0057$, *RDS1*; $P = 0.0008$, FIG4/*LEM3*; $P = 0.0072$, *GUP2*; $P = 0.0030$, *CEN3*) followed by Tukey post test (all pairwise comparisons of means). Error bars show average deviation of two biological repeats.

suggesting that Cse4 K215/216 sumoylation facilitates its deposition into chromatin. Support for this conclusion is based on finding that Cse4 K215/216R exhibits: (1) reduced sumoylation; (2) lack of SDL in *psh1*Δ, *slx5*Δ, and *hir2*Δ strains; (3) reduced interaction with histone chaperones Cac2 and Scm3; and (4) reduced localization to centromeric and to noncentromeric regions. Consistent with a role for Cse4 K215/216 sumoylation in facilitating deposition of Cse4 into chromatin, overexpressed Cse4 K215/216R was unable to suppress the growth of strains depleted of Scm3.

We previously identified and defined a role for sumoylation of Cse4 K65 in the N terminus for proteolysis of Cse4 in preventing its mislocalization (Ohkuni *et al.* 2018). To distinguish the functional roles of K65 and K215/216 sumoylation, we analyzed a triple mutant Cse4 K65/215/216R. The phenotypes of *cse4 K65/215/216R* including lack of *GAL-CSE4* SDL in *psh1*Δ, *slx5*Δ, and *hir2*Δ strains, reduced interaction with Cac2 and Scm3, and reduced localization to centromeric and noncentromeric regions, are not significantly different from those observed for the double mutant

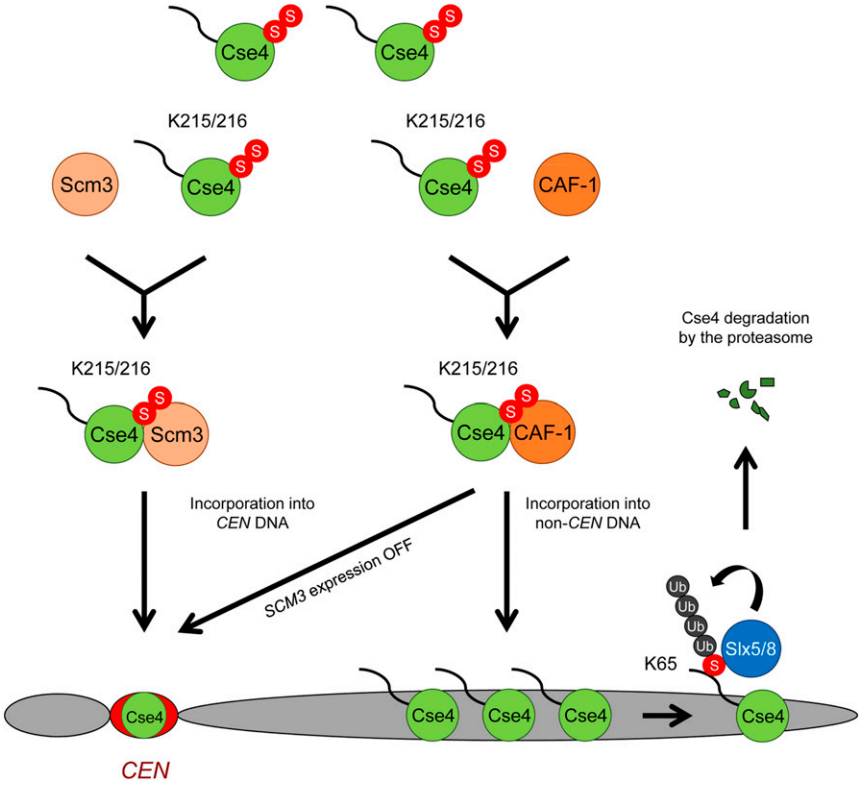

Figure 9 Sumoylation of Cse4 K215/216 facilitates deposition into chromatin. We propose a model in which Cse4 K215/216 sumoylation regulates its interaction with histone chaperones Scm3 and CAF-1, and this facilitates the deposition of overexpressed Cse4 into *CEN* and non-*CEN* regions, respectively. The interaction of sumoylated Cse4 K215/216 with CAF-1 promotes centromeric localization of overexpressed Cse4 only under conditions when Scm3 is depleted (*SCM3* expression OFF). The functional role of Cse4 K215/216 sumoylation is distinct from that of Cse4 K65 sumoylation and Cse4 K65 sumoylation occurs downstream of Cse4 K215/216 sumoylation, *i.e.*, after Cse4 is incorporated into chromatin. Sumoylation of mislocalized Cse4 at K65 promotes its interaction with Slx5 leading to ubiquitin-mediated proteolysis of Cse4 that prevents the stable association of mislocalized Cse4 at non-*CEN* regions (Ohkuni *et al.* 2018).

cse4 K215/216R, but the phenotypes due to *K65R* are suppressed by mutations at K215/216. Hence, the functional role of Cse4 K215/216 sumoylation is distinct from that of Cse4 K65 sumoylation and Cse4 K65 sumoylation occurs downstream of Cse4 K215/216 sumoylation, *i.e.*, after Cse4 is incorporated into chromatin. We propose a model in which Cse4 K215/216 sumoylation regulates its interaction with histone chaperones Scm3 and CAF-1 and this facilitates the deposition of overexpressed Cse4 into *CEN* and non-*CEN* regions, respectively (Figure 9). The interaction of sumoylated Cse4 K215/216 with CAF-1 promotes centromeric localization of overexpressed Cse4 only under conditions when Scm3 is depleted ($Scm3^{off}$). Sumoylation of mislocalized Cse4 at K65 promotes its interaction with Slx5 leading to ubiquitin-mediated proteolysis of Cse4 that prevents the stable association of mislocalized Cse4 at non-*CEN* regions. Overexpressed Cse4 is mislocalized to noncentromeric regions only when proteolytic mechanisms are disrupted.

Though technical difficulties precluded us from conclusively establishing that Cse4 K65 and K215/216 are the direct targets of sumoylation, the phenotypes of *cse4 K215/216R* mutants support a role for these sites in Cse4 sumoylation and not ubiquitination. For example, (1) Cse4 K65 and Cse4 K215/216 meet the criterion for sumoylation consensus motif and Cse4 K65R, Cse4 K215/216R showed reduced levels of sumoylation when compared to wild-type Cse4; (2) Cse4 K65/215/216R showed significantly reduced levels of sumoylation when compared to Cse4 K65R and Cse4 K215/216R; (3) sumoylation of Cse4 is barely detectable in a *siz1*Δ *siz2*Δ strain; (4) *GAL-cse4 K215/216R* does not exhibit SDL in *psh1*Δ and *slx5*Δ strains; (5) Cse4 K215/216 are unlikely to be sites for ubiquitination as previous studies showed ubiquitination of Cse4 K131, K155, K163, and K172 (Hewawasam *et al.* 2010); and (6) Cse4 K215/216R/A does not exhibit defects in Cse4 proteolysis in contrast to Cse4 4KA [K131, K155, K163, K172 mutated to alanine (A)], which exhibits defects in Cse4 proteolysis (Hewawasam *et al.* 2010).

To examine the role of C-terminal sumoylation of Cse4, we constructed Cse4 K215/216R/A mutants. The substitution of K with R preserves the positive charge and since arginine is also target of methylation, we also generated a Cse4 K215/216A mutant. As described above, K-to-A substitutions in Cse4 have been used for studies with Psh1 (Hewawasam *et al.* 2010). Our results showed that even though both *GAL-cse4 K215/216R* and *GAL-cse4 K215/216A* do not exhibit SDL in a *psh1*Δ strain, the growth with *GAL-cse4 K215/216A* is better than that with *GAL-cse4 K215/216R*. Consistent with this, we observed greater defects in the interaction of Cse4 K215/216A with Cac2 and Scm3 and reduced association with noncentromeric and centromeric chromatin when compared to that observed for Cse4 K215/216R. Furthermore, *cse4 K215/216A* expressed from its own promoter has a higher chromosome loss when compared to *cse4 K215/216R* strain under normal physiological conditions. We propose that structural differences between Cse4 K215/216R and Cse4 K215/216A contribute to the difference in the severity of the phenotypes between these two mutants.

Reduced interaction of Cse4 K215/216R and Cse4 K65/215/216R with Cac2 and Scm3 was observed when Cse4 was overexpressed, suggesting that sumoylation Cse4 K215/216 regulates its interaction with histone chaperones. SUMO-interacting motif (SIM) has been identified in several noncovalent interaction partners. For example, Slx5 interacts with sumoylated substrates noncovalently through multiple SIMs (Xie *et al.* 2007; Xie *et al.* 2010). Interestingly, CAF-1 subunits, Cac1 (114-IIAIE-118, $P = 0.019$), Cac2 (271-LVVIP-275, $P = 0.017$), Cac3 (239-IIDLP-243, $P = 0.06$), and Scm3 (161-IIDIS-165, $P = 0.039$) have putative SIMs based on the search engine (GPS-SUMO: http://sumosp.biocuckoo.org; Ren *et al.* 2009; Zhao *et al.* 2014). Future studies will allow us to examine the biological role of individual SIMs in CAF-1 and Scm3 for interaction with Cse4. In addition, the histone chaperone DAXX, which contributes to mislocalization of CENP-A, also has a SIM in the C terminus and this motif is crucial for targeting DAXX to promyelocytic leukemia oncogenic domains (Lin *et al.* 2006). CENP-A in *Arabidopsis* is sumoylated and this sumoylation regulates the disassembly of centromeres, which is a property of terminated differentiated cells (Mérai *et al.* 2014). It will be of interest to determine if human CENP-A is sumoylated and if sumoylation of CENP-A regulates its interaction with DAXX in human cells. These studies are clinically relevant because mutations in DAXX predict better prognosis of pancreatic neuroendocrine tumors. Additionally, overexpression and depletion of DAXX correlates with an enhancement or suppression of ovarian cancer cell proliferation, respectively.

In conclusion, our studies provide the first evidence for sumoylation of Cse4 K215/216 and a possible mechanistic role of Cse4 sumoylation for interaction with Scm3 and CAF-1 thereby facilitating Cse4 deposition into chromatin. We propose that when overexpressed, high levels of sumoylated Cse4 are mislocalized, and this contributes in part to the SDL of *GAL-CSE4* in mutants such as *psh1*Δ, *hir2*Δ, and *slx5*Δ that are defective in Cse4 proteolysis. Additionally, our data shows that the biological role of Cse4 K215/216 sumoylation in facilitating chromatin deposition is independent of the role of Cse4 K65 sumoylation in regulating Cse4 proteolysis. Since all canonical histones are sumoylated (Nathan *et al.* 2006) and histone chaperones such as HJURP and CAF-1 are well conserved, we also propose that sumoylation of histones and histone variants is critical for their interaction with chaperones and chromatin-associated functions. Our results provide impetus for future studies to further understand how Cse4 sumoylation regulates chromosomal stability when the balance of chromatin-associated Cse4 and H3 is altered. Furthermore, characterization of pathways that regulate deposition of overexpressed Cse4 will help us to understand mechanisms that promote mislocalization of CENP-A in human cancers.

Acknowledgments

We gratefully acknowledge Jennifer Gerton for strains, Brian D. Strahl for a rabbit anti-Cse4 antibody, Michael Matunis and members of the Basrai laboratory for helpful discussions. This work was supported by the National Institutes of Health Intramural Research Program to M.A.B.

Author contributions: K.O. designed the study, conducted most of the experiments, analyzed the data, and wrote the manuscript. E.S. assisted with biochemical experiments and growth assays. W.-C.A. generated plasmids and provided technical advice. R.L.-M. contributed to sumoylation assays. R.L.W. and P.S.M. performed ChIP-sequencing experiments. R.E.B. analyzed ChIP-sequencing data and contributed to the writing of the manuscript. M.A.B. guided the project and contributed to the writing of the manuscript.

Literature Cited

Amato, A., T. Schillaci, L. Lentini, and A. Di Leonardo, 2009 CENPA overexpression promotes genome instability in pRb-depleted human cells. Mol. Cancer 8: 119. https://doi.org/10.1186/1476-4598-8-119

Athwal, R. K., M. P. Walkiewicz, S. Baek, S. Fu, M. Bui *et al.*, 2015 CENP-A nucleosomes localize to transcription factor hotspots and subtelomeric sites in human cancer cells. Epigenetics Chromatin 8: 2. https://doi.org/10.1186/1756-8935-8-2

Au, W. C., M. J. Crisp, S. Z. DeLuca, O. J. Rando, and M. A. Basrai, 2008 Altered dosage and mislocalization of histone H3 and Cse4p lead to chromosome loss in *Saccharomyces cerevisiae*. Genetics 179: 263–275. https://doi.org/10.1534/genetics.108.088518

Au, W. C., A. R. Dawson, D. W. Rawson, S. B. Taylor, R. E. Baker *et al.*, 2013 A novel role of the N terminus of budding yeast histone H3 variant Cse4 in ubiquitin-mediated proteolysis. Genetics 194: 513–518. https://doi.org/10.1534/genetics.113.149898

Au, W. C., T. Zhang, P. K. Mishra, J. R. Eisenstatt, R. L. Walker *et al.*, 2020 Skp, Cullin, F-box (SCF)-Met30 and SCF-Cdc4-Mediated proteolysis of CENP-A prevents mislocalization of CENP-A for chromosomal stability in budding yeast. PLoS Genet. 16: e1008597. https://doi.org/10.1371/journal.pgen.1008597

Bernier-Villamor, V., D. A. Sampson, M. J. Matunis, and C. D. Lima, 2002 Structural basis for E2-mediated SUMO conjugation revealed by a complex between ubiquitin-conjugating enzyme Ubc9 and RanGAP1. Cell 108: 345–356. https://doi.org/10.1016/S0092-8674(02)00630-X

Biggins, S., 2013 The composition, functions, and regulation of the budding yeast kinetochore. Genetics 194: 817–846. https://doi.org/10.1534/genetics.112.145276

Boltengagen, M., A. Huang, A. Boltengagen, L. Trixl, H. Lindner *et al.*, 2016 A novel role for the histone acetyltransferase Hat1 in the CENP-A/CID assembly pathway in *Drosophila melanogaster*. Nucleic Acids Res. 44: 2145–2159. https://doi.org/10.1093/nar/gkv1235

Camahort, R., B. Li, L. Florens, S. K. Swanson, M. P. Washburn *et al.*, 2007 Scm3 is essential to recruit the histone h3 variant cse4 to centromeres and to maintain a functional kinetochore. Mol. Cell 26: 853–865. https://doi.org/10.1016/j.molcel.2007.05.013

Camahort, R., M. Shivaraju, M. Mattingly, B. Li, S. Nakanishi *et al.*, 2009 Cse4 is part of an octameric nucleosome in budding yeast. Mol. Cell 35: 794–805. https://doi.org/10.1016/j.molcel.2009.07.022

Cheng, H., X. Bao, X. Gan, S. Luo, and H. Rao, 2017 Multiple E3s promote the degradation of histone H3 variant Cse4. Sci. Rep. 7: 8565. https://doi.org/10.1038/s41598-017-08923-w

Ciftci-Yilmaz, S., W. C. Au, P. K. Mishra, J. R. Eisenstatt, J. Chang *et al.*, 2018 A genome-wide screen reveals a role for the HIR

histone chaperone complex in preventing mislocalization of budding yeast CENP-A. Genetics 210: 203–218. https://doi.org/10.1534/genetics.118.301305

Collins, K. A., S. Furuyama, and S. Biggins, 2004 Proteolysis contributes to the exclusive centromere localization of the yeast Cse4/CENP-A histone H3 variant. Curr. Biol. 14: 1968–1972. https://doi.org/10.1016/j.cub.2004.10.024

Fujita, Y., T. Hayashi, T. Kiyomitsu, Y. Toyoda, A. Kokubu *et al.*, 2007 Priming of centromere for CENP-A recruitment by human hMis18alpha, hMis18beta, and M18BP1. Dev. Cell 12: 17–30. https://doi.org/10.1016/j.devcel.2006.11.002

Heun, P., S. Erhardt, M. D. Blower, S. Weiss, A. D. Skora *et al.*, 2006 Mislocalization of the *Drosophila* centromere-specific histone CID promotes formation of functional ectopic kinetochores. Dev. Cell 10: 303–315. https://doi.org/10.1016/j.devcel.2006.01.014

Hewawasam, G., M. Shivaraju, M. Mattingly, S. Venkatesh, S. Martin-Brown *et al.*, 2010 Psh1 is an E3 ubiquitin ligase that targets the centromeric histone variant Cse4. Mol. Cell 40: 444–454. https://doi.org/10.1016/j.molcel.2010.10.014

Hewawasam, G. S., K. Dhatchinamoorthy, M. Mattingly, C. Seidel, and J. L. Gerton, 2018 Chromatin assembly factor-1 (CAF-1) chaperone regulates Cse4 deposition into chromatin in budding yeast. Nucleic Acids Res. 46: 4440–4455 (erratum: Nucleic Acids Res. 46: 4831). https://doi.org/10.1093/nar/gky169

Hildebrand, E. M., and S. Biggins, 2016 Regulation of budding yeast CENP-A levels prevents misincorporation at promoter nucleosomes and transcriptional defects. PLoS Genet. 12: e1005930. https://doi.org/10.1371/journal.pgen.1005930

Hu, Z., G. Huang, A. Sadanandam, S. Gu, M. E. Lenburg *et al.*, 2010 The expression level of HJURP has an independent prognostic impact and predicts the sensitivity to radiotherapy in breast cancer. Breast Cancer Res. 12: R18. https://doi.org/10.1186/bcr2487

Kitagawa, K., and P. Hieter, 2001 Evolutionary conservation between budding yeast and human kinetochores. Nat. Rev. Mol. Cell Biol. 2: 678–687. https://doi.org/10.1038/35089568

Lacoste, N., A. Woolfe, H. Tachiwana, A. V. Garea, T. Barth *et al.*, 2014 Mislocalization of the centromeric histone variant CenH3/CENP-A in human cells depends on the chaperone DAXX. Mol. Cell 53: 631–644. https://doi.org/10.1016/j.molcel.2014.01.018

Lin, D. Y., Y. S. Huang, J. C. Jeng, H. Y. Kuo, C. C. Chang *et al.*, 2006 Role of SUMO-interacting motif in Daxx SUMO modification, subnuclear localization, and repression of sumoylated transcription factors. Mol. Cell 24: 341–354. https://doi.org/10.1016/j.molcel.2006.10.019

Li, Y., Z. Zhu, S. Zhang, D. Yu, H. Yu *et al.*, 2011 ShRNA-targeted centromere protein A inhibits hepatocellular carcinoma growth. PLoS One 6: e17794. https://doi.org/10.1371/journal.pone.0017794

Lopes da Rosa, J., J. Holik, E. M. Green, O. J. Rando, and P. D. Kaufman, 2011 Overlapping regulation of CenH3 localization and histone H3 turnover by CAF-1 and HIR proteins in *Saccharomyces cerevisiae*. Genetics 187: 9–19. https://doi.org/10.1534/genetics.110.123117

McKinley, K. L., and I. M. Cheeseman, 2016 The molecular basis for centromere identity and function. Nat. Rev. Mol. Cell Biol. 17: 16–29. https://doi.org/10.1038/nrm.2015.5

Mérai, Z., N. Chumak, M. Garcia-Aguilar, T. F. Hsieh, T. Nishimura *et al.*, 2014 The AAA-ATPase molecular chaperone Cdc48/p97 disassembles sumoylated centromeres, decondenses heterochromatin, and activates ribosomal RNA genes. Proc. Natl. Acad. Sci. USA 111: 16166–16171. https://doi.org/10.1073/pnas.1418564111

Mizuguchi, G., H. Xiao, J. Wisniewski, M. M. Smith, and C. Wu, 2007 Nonhistone Scm3 and histones CenH3–H4 assemble the core of centromere-specific nucleosomes. Cell 129: 1153–1164. https://doi.org/10.1016/j.cell.2007.04.026

Moreno-Moreno, O., M. Torras-Llort, and F. Azorin, 2006 Proteolysis restricts localization of CID, the centromere-specific histone H3 variant of *Drosophila*, to centromeres. Nucleic Acids Res. 34: 6247–6255. https://doi.org/10.1093/nar/gkl902

Nathan, D., K. Ingvarsdottir, D. E. Sterner, G. R. Bylebyl, M. Dokmanovic *et al.*, 2006 Histone sumoylation is a negative regulator in *Saccharomyces cerevisiae* and shows dynamic interplay with positive-acting histone modifications. Genes Dev. 20: 966–976. https://doi.org/10.1101/gad.1404206

Ohkuni, K., Y. Takahashi, and M. A. Basrai, 2015 Protein purification technique that allows detection of sumoylation and ubiquitination of budding yeast kinetochore proteins Ndc10 and Ndc80. J. Vis. Exp. (99): e52482. https://doi.org/https://doi.org/10.3791/52482

Ohkuni, K., Y. Takahashi, A. Fulp, J. Lawrimore, W. C. Au *et al.*, 2016 SUMO-Targeted Ubiquitin Ligase (STUbL) Slx5 regulates proteolysis of centromeric histone H3 variant Cse4 and prevents its mislocalization to euchromatin. Mol. Biol. Cell 27(9): 1500–1510. https://doi.org/10.1091/mbc.E15-12-0827

Ohkuni, K., R. Levy-Myers, J. Warren, W. C. Au, Y. Takahashi *et al.*, 2018 N-terminal sumoylation of centromeric histone H3 variant Cse4 regulates its proteolysis to prevent mislocalization to non-centromeric chromatin. G3 (Bethesda) 8: 1215–1223. https://doi.org/10.1534/g3.117.300419

Pidoux, A. L., E. S. Choi, J. K. Abbott, X. Liu, A. Kagansky *et al.*, 2009 Fission yeast Scm3: a CENP-A receptor required for integrity of subkinetochore chromatin. Mol. Cell 33: 299–311. https://doi.org/10.1016/j.molcel.2009.01.019

Ranjitkar, P., M. O. Press, X. Yi, R. Baker, M. J. MacCoss *et al.*, 2010 An E3 ubiquitin ligase prevents ectopic localization of the centromeric histone H3 variant via the centromere targeting domain. Mol. Cell 40: 455–464. https://doi.org/10.1016/j.molcel.2010.09.025

Ren, J., X. Gao, C. Jin, M. Zhu, X. Wang *et al.*, 2009 Systematic study of protein sumoylation: development of a site-specific predictor of SUMOsp 2.0. Proteomics 9: 3409–3412. https://doi.org/10.1002/pmic.200800646

Rodriguez, M. S., C. Dargemont, and R. T. Hay, 2001 SUMO-1 conjugation in vivo requires both a consensus modification motif and nuclear targeting. J. Biol. Chem. 276: 12654–12659. https://doi.org/10.1074/jbc.M009476200

Sampson, D. A., M. Wang, and M. J. Matunis, 2001 The small ubiquitin-like modifier-1 (SUMO-1) consensus sequence mediates Ubc9 binding and is essential for SUMO-1 modification. J. Biol. Chem. 276: 21664–21669. https://doi.org/10.1074/jbc.M100006200

Shrestha, R. L., G. S. Ahn, M. I. Staples, K. M. Sathyan, T. S. Karpova *et al.*, 2017 Mislocalization of centromeric histone H3 variant CENP-A contributes to chromosomal instability (CIN) in human cells. Oncotarget 8: 46781–46800. https://doi.org/10.18632/oncotarget.18108

Spencer, F., S. L. Gerring, C. Connelly, and P. Hieter, 1990 Mitotic chromosome transmission fidelity mutants in *Saccharomyces cerevisiae*. Genetics 124: 237–249.

Stoler, S., K. Rogers, S. Weitze, L. Morey, M. Fitzgerald-Hayes *et al.*, 2007 Scm3, an essential *Saccharomyces cerevisiae* centromere protein required for G2/M progression and Cse4 localization. Proc. Natl. Acad. Sci. USA 104: 10571–10576. https://doi.org/10.1073/pnas.0703178104

Sun, X., P. L. Clermont, W. Jiao, C. D. Helgason, P. W. Gout *et al.*, 2016 Elevated expression of the centromere protein-A(CENP-A)-encoding gene as a prognostic and predictive biomarker in human cancers. Int. J. Cancer 139: 899–907. https://doi.org/10.1002/ijc.30133

Tomonaga, T., K. Matsushita, S. Yamaguchi, T. Oohashi, H. Shimada *et al.*, 2003 Overexpression and mistargeting of centromere protein-A in human primary colorectal cancer. Cancer Res. 63: 3511–3516.

Williams, J. S., T. Hayashi, M. Yanagida, and P. Russell, 2009 Fission yeast Scm3 mediates stable assembly of Cnp1/CENP-A into centromeric chromatin. Mol. Cell 33: 287–298. https://doi.org/10.1016/j.molcel.2009.01.017

Wu, Q., Y. M. Qian, X. L. Zhao, S. M. Wang, X. J. Feng *et al.*, 2012 Expression and prognostic significance of centromere protein A in human lung adenocarcinoma. Lung Cancer 77: 407–414. https://doi.org/10.1016/j.lungcan.2012.04.007

Xie, Y., O. Kerscher, M. B. Kroetz, H. F. McConchie, P. Sung *et al.*, 2007 The yeast Hex3.Slx8 heterodimer is a ubiquitin ligase stimulated by substrate sumoylation. J. Biol. Chem. 282: 34176–34184. https://doi.org/10.1074/jbc.M706025200

Xie, Y., E. M. Rubenstein, T. Matt, and M. Hochstrasser, 2010 SUMO-independent in vivo activity of a SUMO-targeted ubiquitin ligase toward a short-lived transcription factor. Genes Dev. 24: 893–903. https://doi.org/10.1101/gad.1906510

Zhao, Q., Y. Xie, Y. Zheng, S. Jiang, W. Liu *et al.*, 2014 GPS-SUMO: a tool for the prediction of sumoylation sites and SUMO-interaction motifs. Nucleic Acids Res. 42: W325–W330. https://doi.org/10.1093/nar/gku383

Communicating editor: J. Nickoloff